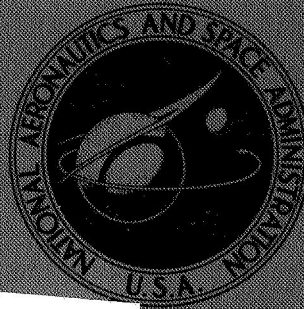


NASA TECHNICAL
MEMORANDUM



NASA TM X-1575

NASA TM X-1575

GPO PRICE \$ _____
CFSTI PRICE(S) \$ _____
Hard copy (HC) 3.00
Microfiche (MF) .65
ff 653 July 65

FACILITY FORM 602

N 68-24245
(ACCESSION NUMBER) (THRU) _____
38
(PAGES) (CODE) _____
✓
(NASA CR OR TMX OR AD NUMBER) (CATEGORY) 02

FLIGHT TEST OF A 40-FOOT-NOMINAL-DIAMETER
DISK-GAP-BAND PARACHUTE DEPLOYED AT A
MACH NUMBER OF 1.91 AND A DYNAMIC PRESSURE
OF 11.6 POUNDS PER SQUARE FOOT

by John S. Preisser and Clinton V. Eckstrom

Langley Research Center

Langley Station, Hampton, Va.



FLIGHT TEST OF A 40-FOOT-NOMINAL-DIAMETER DISK-GAP-BAND
PARACHUTE DEPLOYED AT A MACH NUMBER OF 1.91 AND A
DYNAMIC PRESSURE OF 11.6 POUNDS PER SQUARE FOOT

By John S. Preisser and Clinton V. Eckstrom

Langley Research Center
Langley Station, Hampton, Va.

Technical Film Supplement L-1000 available on request.

NATIONAL AERONAUTICS AND SPACE ADMINISTRATION

For sale by the Clearinghouse for Federal Scientific and Technical Information
Springfield, Virginia 22151 - CFSTI price \$3.00

FLIGHT TEST OF A 40-FOOT-NOMINAL-DIAMETER DISK-GAP-BAND
PARACHUTE DEPLOYED AT A MACH NUMBER OF 1.91 AND A
DYNAMIC PRESSURE OF 11.6 POUNDS PER SQUARE FOOT

By John S. Preisser and Clinton V. Eckstrom
Langley Research Center

SUMMARY

A 40-foot (12.2 meter) nominal-diameter disk-gap-band parachute was flight tested as part of the NASA Supersonic Planetary Entry Decelerator Program (SPED-I). The test parachute was ejected by a deployment mortar from an instrumented payload at an altitude of 140 000 feet (42.5 kilometers). The payload was at a Mach number of 1.91 and the dynamic pressure was 11.6 pounds per square foot (555 newtons per square meter) at the time the parachute deployment mortar was fired. The parachute reached suspension line stretch in 0.43 second with a resultant snatch force loading of 1990 pounds (8850 newtons). The maximum parachute opening load of 6500 pounds (28 910 newtons) came 0.61 second later at a total elapsed time from mortar firing of 1.04 seconds. The first full inflation occurred at 1.12 seconds and stable inflation was achieved at approximately 1.60 seconds. The parachute had an average axial-force coefficient of 0.53 during the deceleration period. During the steady-state descent portion of the flight test, the average effective drag coefficient was also 0.53 and pitch-yaw oscillations of the canopy averaged less than 10^0 in the altitude region above 100 000 feet (30.5 meters). Examination of the recovered parachute revealed that it had not been damaged during the flight test.

INTRODUCTION

In recent years there has been renewed and expanded interest in parachutes for decelerating scientific payloads. Extended requirements include such applications as proposed experiments in planetary atmospheres and the lowering of sounding rocket instrumentation through high-altitude regions above the earth. Parachute experiments initiated at deployment conditions of supersonic velocities and relatively low dynamic pressures had not been previously conducted. In addition, drag and stability characteristics of parachutes in a low pressure and density environment has been relatively unknown. In recognition of this deficiency in existing technology, the Planetary Entry Parachute Program (PEPP) was established at the NASA Langley Research Center

(ref. 1). Earlier publications containing results from this program are listed as references 2 to 9. In order to achieve a higher test Mach number at the same dynamic pressure, an additional stage was added to the vehicle system for the rocket-launched tests of PEPP and the program renamed Supersonic Planetary Entry Decelerator Program (SPED-I). This report concerns the first of these latter tests.

Results are presented herein from a test of a 40-foot-nominal-diameter (12.2 meter) parachute of disk-gap-band configuration. Prior to this test, 30- and 64.5-foot-nominal-diameter (9.1 and 19.7 meter) disk-gap-band parachutes had been tested in the PEPP series (refs. 2 and 3). The desired deployment conditions for this test were a Mach number of 2.0 and a dynamic pressure of 10 pounds per square foot (479 newtons per square meter).

As was the case for all PEPP tests, SPED-I test objectives were to observe the dynamics of the parachute deployment and inflation and to measure opening shock loads, parachute drag efficiency, and stability characteristics.

Motion-picture film supplement L-1000 is available on loan; a request card and a description of the film are included at the back of this paper.

SYMBOLS

$C_{A,o}$	axial-force coefficient, $\frac{m_{\text{total}}}{m_{\text{payload}}} \frac{T}{q_{\infty} S_o}$
$(C_{D,o})_{\text{eff}}$	effective drag coefficient (based on vertical descent velocity and acceleration)
D_o	nominal diameter, $\left(\frac{4S_o}{\pi}\right)^{1/2}$, feet (meters)
g	acceleration due to gravity, 32.2 feet/second ² (9.80665 meters/second ²)
M	Mach number
m	mass, slugs (kilograms)
q_{∞}	free-stream dynamic pressure, $\frac{1}{2}\rho_{\infty} V^2$, pound/foot ² (newtons/meter ²)
S_o	nominal surface area of parachute canopy including the gap and vent, feet ² (meters ²)

S_p	projected area of parachute canopy, feet ² (meters ²)
T	tensiometer force, pounds (newtons)
t	time from vehicle lift-off, seconds
t'	time from mortar firing, seconds
V	true airspeed, feet/second (meters/second)
X, Y, Z	payload body-axis system
X_f, Y_f, Z_f	earth-fixed axis system (refer to fig. 19)
Z_E	local vertical axis
δ_E	payload resultant pitch-yaw angle from the local vertical, degrees
θ_g, ψ_g, ϕ_g	gyro platform angles relating body-axis system to inertial coordinate system (vehicle lift-off position), degrees
θ_E, ψ_E, ϕ_E	Euler angles relating body-axis system to earth-fixed axis system, degrees (refer to fig. 19)
ρ_∞	free-stream atmospheric density, slugs/foot ³ (kilograms/meter ³)

Dots over symbols denote differentiation with respect to time. Bars over symbols denote mean values averaged on a cycle-to-cycle basis.

TEST SYSTEM DESCRIPTION

The payload was carried to the test point by means of an Honest John-Nike-Nike rocket vehicle. A photograph of the vehicle configuration is presented in figure 1. A brief discussion of the launch-vehicle system used in PEPP testing has been presented in reference 5. With the exception of the additional third-stage Nike rocket motor, the SPED-I launch-vehicle system was identical. To initiate parachute deployment, a radio command system was used to start a programmer which, in turn, initiated the firing of a deployment mortar. A real-time visual display of the variation of velocity with altitude for the payload, which incorporated grids of constant Mach number and dynamic

pressure, such as is described in references 1 and 5, was used as a guide to determine the proper time for transmitting the radio command signal.

A diagram of the test payload is presented in figure 2. Onboard instrumentation consisted of an electrical strain-gage type tensiometer located in the parachute riser line, a $\pm 75g$ range accelerometer located approximately 1 foot forward of the center of gravity of the instrumented payload and aligned with the longitudinal axis and two $\pm 5g$ range accelerometers mounted normal to each other and perpendicular to the longitudinal axis. An attitude reference system, commonly referred to as a gyro platform, was included to record payload motions in pitch, yaw, and roll. In addition, a camera was mounted in a pod on the payload (fig. 2) and pointed aft to view the parachute performance while a second camera was mounted in the nose of the payload and pointed forward. The tensiometer, accelerometer, and gyro-platform measurements were telemetered to ground receiving stations and recorded on magnetic tape. Camera film was obtained from the recovered payload. Timing indications for use in correlating the telemetered data and the camera film were obtained by means of a coded timer.

In addition to the data-gathering instrumentation, a C-band transponder was included in the payload to facilitate radar tracking as well as a homing beacon to aid in recovery operations. The payload also contained two auxiliary parachutes which could be deployed by radio command at any time after payload separation if the performance of the test parachute was such that the descent velocity was high and damage would most likely occur to the payload upon impact. (For reasons of economy, payloads recovered in good condition were refurbished and used again in subsequent flights.)

TEST PARACHUTE DESCRIPTION

The test parachute was a disk-gap-band (DGB) design having a nominal diameter D_0 of 40 feet (12.2 meters) and a reference area S_0 of 1256 square feet (116 square meters). (The reference area is taken to include the gap and vent area as well as that of the disk and the band.) Figure 3 presents the dimensional details of a gore and the general parachute-payload configuration. The in-flight diameter of the test parachute was estimated to be approximately 27 feet (8.2 meters). The parachute had a total geometric porosity or open area of 12.5 percent. The gap provided a geometric porosity of 12 percent and the apex vent opening provided the additional 0.5-percent geometric porosity.

The test parachute had 32 gores and was fabricated entirely of dacron materials. The suspension lines were coreless braided dacron having a rated tensile strength of 550 pounds (2450 newtons). The canopy disk and band gore panels were fabricated of 2.0 ounce-per-square-yard (68 grams per square meter) dacron cloth of rip-stop design. There were three panels in the disk portion and two panels in the band portion of each

gore. (See fig. 3.) The gore panels were fabricated with the material warp and fill threads running 45° to the center line of the gore.

The canopy was reinforced at various places with 3/4-inch (1.91 cm) wide dacron tape having a rated tensile strength of 550 pounds (2450 newtons). The vent edge was reinforced with two thicknesses of tape. The outer edge of the disk and both edges of the band were reinforced with a single thickness of tape. The gore edges were joined by a french-fell seam and reinforced with a load tape (referred to as a radial tape) which was continuous up the full length of a gore, across the vent, and down the gore seam on the opposite side of the canopy. At the lower edge of the band, the radial tape was made to form a loop and was sewn back 4 inches (10.2 cm) on the inside surface of the band. This loop was used for attachment of the suspension lines. The radial tape was a double thickness across the gap between the band and the disk.

The parachute-attachment system consisted of an upper riser, a swivel, an intermediate riser, a tensiometer, and a bridle. Both the upper and intermediate riser were constructed of four layers of dacron webbing, each having a rated tensile strength of 6000 pounds (26 800 newtons), whereas the bridle was constructed of three layers of nylon webbing having a 10 000-pound (44 480 newton) tensile strength. The upper riser was 4 feet (1.2 meters) in length, the tensiometer and the swivel were each approximately 1/2 foot (15 cm) long, the intermediate riser was 2 feet (0.61 meter) in length and the bridle was $4\frac{1}{2}$ feet (1.37 meters) long; thus, the total length of the attachment system was $11\frac{1}{2}$ feet (3.5 meters).

The parachute was equipped with the additional lines and reefing rings necessary for a post-reefing operation. A description of this system can be found in reference 6. The post-reefing system was not activated for this flight test.

The parachute canopy, suspension lines, post-reefing lines and rings, and upper riser weighed 34 pounds (15.4 kilograms). The swivel, intermediate riser, attachment pins, bushings and rings weighed 3.0 pounds (1.4 kilograms); thus, the total parachute assembly weight was 37.0 pounds (16.8 kilograms). The tensiometer and bridle weights were included as part of the payload weight which was 243 pounds (110 kilograms). Thus the total weight of the payload-parachute system during descent was 280 pounds (127 kilograms).

The parachute was packed in a cylindrical deployment bag of dacron canvas which was lined with teflon cloth to reduce friction during packing and deployment. The parachute was packed in the deployment bag to a density of 40 lb/ft³ (641 kg/m³). The open end of the bag had overlapping closure flaps which were held in the closed position with a tie cord. This tie cord was severed during the deployment by a circular knife located on the main parachute riser. No canopy or suspension line holders or restraints were

used inside the deployment bag except for a 300-pound (1330-newton) break line from the apex of the canopy to the bottom of the bag.

The packed parachute and deployment bag were subjected to a temperature of 125° C for 120 hours. This heat cycle is representative of part of the sterilization requirements for equipment to be used in interplanetary spacecraft and therefore was included as part of the test requirements so that any resulting effects on deployment, structural strength, or shrinkage would exist for these tests.

RESULTS AND DISCUSSION

Test Data

The flight-test vehicle was launched at 9:32 a.m. mdt on September 19, 1967, at White Sands Missile Range, New Mexico. Figure 4 presents the flight sequence and the recorded times for significant flight events. Time histories of altitude and relative velocity for the first 360 seconds of the flight are shown in figure 5. As was the case for all flights in the PEPP series, the payload was in the ascent portion of the flight trajectory at the time the parachute was deployed ($t = 70.17$ seconds).

An Arcas meteorological sounding rocket was launched 1 hour after the flight test to measure upper-altitude winds and temperatures. This information was supplemented by a rawinsonde released 15 minutes prior to the flight test. Upper atmosphere winds as determined from the rocket sounding are presented in figure 6. Atmospheric density as derived from the measured temperatures of both soundings is presented in figure 7.

The measured atmospheric data were used with radar track and tensiometer data to determine time histories of payload true airspeed and Mach number (fig. 8) and dynamic pressure (fig. 9). By definition, the initiation of the deployment sequence or time of deployment corresponds to mortar firing ($t' = 0$ in the figures). Thus, as can be seen in figures 8 and 9, parachute deployment was initiated at a true airspeed of 2030 feet per second (616 meters per second) or $M = 1.91$ and a dynamic pressure of 11.6 pounds per square foot (555 newtons per square meter). The deployment altitude was 140 000 feet (42.5 kilometers) above mean sea level. A time history of altitude for the parachute-payload system including the deployment sequence, as determined by radar tracking, is presented in figure 10.

The time history of force transmitted through the riser line as measured by the tensiometer during the primary test period is presented in figure 11. The peak load of 870 pounds (3870 newtons) at $t' = 0.17$ second is attributed to full-length deployment of the parachute riser system. The peak force of 1990 pounds (8850 newtons) at $t' = 0.43$ second was the snatch force associated with stretching of the suspension lines.

The largest peak force of 6500 pounds (28 910 newtons) at $t' = 1.04$ seconds occurred during the parachute opening process.

Figure 12 presents the data obtained from the three accelerometers located in the payload. Positive longitudinal accelerations imposed by the firing of the mortar are not shown but were an average of 30g for 0.02-second duration. Deceleration loads determined by the longitudinal accelerometer measurement are in close agreement with those recorded by the tensiometer.

Analysis of Parachute Performance

Inflation characteristics.- The test parachute was deployed from the payload at an average ejection velocity of 120 feet per second (36.5 meters per second) based on the constructed suspension line plus attachment system length of 51.5 feet (15.7 meters) and a time to line stretch of 0.43 second. As mentioned previously, the resulting snatch force was 1990 pounds (8850 newtons).

Selected frames from the payload aft camera film showing parachute deployment, canopy inflation, canopy shape changes, and steady full canopy inflation (shown at apogee) are presented in figure 13. The disk portion of the canopy appears to be inflated fully for the first time at $t' = 0.80$ second and the entire canopy appears inflated fully for the first time at $t' = 1.12$ seconds. The band portion of the canopy continued to flutter slightly until $t' = 1.6$ seconds; after this time only minor variations in canopy shape were observed. Variation with time of the ratio of the parachute projected area S_p to the projected area presented by the fully opened parachute $S_{p,final}$ is presented in figure 14.

Drag efficiency.- A computed axial-force coefficient $C_{A,o}$ is presented in figure 15 as a function of time from mortar deployment. In addition to the time scale, a Mach number scale is also shown for reference. The equation used to derive this force coefficient is as follows:

$$C_{A,o} = \frac{m_{total}}{m_{payload}} \frac{T}{q_{\infty} S_o}$$

The relatively large variations in $C_{A,o}$ which exist prior to 1.6 seconds reflect the variations found in the tensiometer-force time history (fig. 11) and can be associated with the rapid changes occurring during the canopy inflation process and during the subsequent flutter of the canopy band. After 1.6 seconds, the canopy remained in a stable inflated condition and variations in $C_{A,o}$ were small. The Mach number of the payload-parachute system at the time stable inflation was achieved was approximately 1.4.

For the relatively steady conditions, such as were experienced during the latter time period of this test, the axial-force coefficient may also be considered to be the parachute drag coefficient during the rather rapid traverse through the Mach number range indicated in figure 15. Once a stable inflation was achieved, an average $C_{A,0}$ of 0.53 was maintained. The estimated uncertainty in this average value, based on a first-order error analysis using a 3-percent density error, 3-percent velocity error, and 100-pound (444.8 newton) tensiometer force uncertainty, was ± 0.04 .

Figure 16 presents the vertical descent velocity and the "effective" drag coefficient variations with altitude. The effective drag coefficient values are based on vertical descent velocity and acceleration and the system weight as shown by the following equation:

$$(C_{D,o})_{\text{eff}} = \frac{2m_{\text{total}}}{\rho_{\infty} \dot{z}_E^2 S_o} (g - \ddot{z}_E)$$

During the descent portion of the flight test, the average effective drag coefficient $(C_{D,o})_{\text{eff}}$ was 0.53 as can be seen in figure 16. The small variations from this average value are within the uncertainty in $(C_{D,o})_{\text{eff}}$ which was estimated to be ± 0.04 when a 3-percent density error, 3-percent velocity error, and 10-percent acceleration error are assumed.

Stability.- It was determined from the gyro platform data that at the time of mortar firing, the payload was rolling at approximately 0.30 revolution per second. As in all previous PEPP tests, the parachute canopy retained very little rolling motion after it became inflated. This result can be seen in figure 17 by comparing the aft-camera film data with gyro-platform or payload roll data which shows that the canopy retained a residual roll rate of approximately 0.02 revolution per second during the deceleration period following deployment. (Relative roll data could not be determined from the camera film between 0 and 1.25 seconds.) Payload pitch and yaw motions during this time period can be seen from figure 18. Pitch angle θ_g and yaw angle ψ_g at $t' = 0$ are measurements of the net pitch and yaw undergone by the payload from the time of gyro uncaging to the time of mortar firing. Pitch and yaw were averaged on a cycle-to-cycle basis; the resulting average values, $\bar{\theta}_g$ and $\bar{\psi}_g$, are represented by the dashed curves in figure 18. As a result of an analysis of the aft camera film data in conjunction with the gyro data (shown by the solid curves in fig. 18), it was determined that $\bar{\theta}_g$ and $\bar{\psi}_g$ represent the motion of the combined payload-parachute system, whereas the oscillatory portion of θ_g and ψ_g resulted from payload motions relative to the parachute center line. System yaw motions were slight; the general increasing trend in $\bar{\theta}_g$ is, of course, due to the payload-parachute system pitching downward as apogee is approached.

During descent, payload motions relative to the parachute center line were small; aft camera film data revealed that over the time interval from $t' = 50$ seconds to $t' = 130$ seconds, the relative angle between the payload and parachute was never greater than 1.5° . Gyro platform data, transformed by the method presented in reference 8 to the Euler angle system shown in figure 19, therefore represents attitude histories of the payload and parachute acting together like a rigid body. Figure 20 presents ψ_E , θ_E , and the magnitude of the resultant angle $|\delta_E|$, over a portion of descent which corresponds to the altitude range from 139 000 to 115 000 feet (42.4 to 35.1 kilometers). The total angular displacement $|\delta_E|$ never exceeded 18° and the average value of this parameter over this interval was less than 10° . The data contained in figure 20 include the effects due to winds. A series of photographs taken from the recovery airplane and showing the descending payload-parachute system shortly before impact is presented in figure 21.

Analysis of recovered parachute.- A postflight examination of the recovered parachute revealed that there was no external damage to the test item. The recovered parachute was measured to determine whether any change in size or constructed shape had resulted from the preflight sterilization heat cycle. It was found that the constructed dimensions of canopy cloth and suspension lines had not changed; however, all canopy structural members, that is, radial tapes, skirt tape, gap-edge tapes, and vent-edge tapes had shrunk about 8 percent in length. Therefore, the nominal area, as defined by the gore-edge tapes, would calculate to be 1065 square feet (99 square meters) which is a reduction of 15 percent from the original area. This reduction in area gives a nominal diameter after shrinkage of 36.8 feet (11.2 meters). The originally constructed canopy area has been used for data analysis in preparation of this report.

CONCLUSIONS

A 40-foot (12.2 meter) nominal-diameter disk-gap-band parachute was deployed at an altitude of 140 000 feet (42.5 kilometers) when the system was at a Mach number of 1.91 and the free-stream dynamic pressure was 11.6 pounds per square foot (555 newtons per square meter). Based on an analysis of the data acquired, the following conclusions are made:

1. The parachute was properly ejected from the payload by the mortar system.
2. The time from initiation of deployment to suspension-line stretch was 0.43 second and the resultant snatch-force loading was 1990 pounds (8850 newtons).
3. The first full inflation occurred at 1.12 seconds and a stable inflation (as evidenced by the derived axial-force coefficient) was achieved at approximately 1.6 seconds.

4. The maximum parachute opening load was 6500 pounds (28 910 newtons) and occurred shortly before first full inflation.

5. The test parachute exhibited an average drag coefficient of 0.53 during both the deceleration period and the descent.

6. The payload-parachute system maintained a relatively stable attitude during the deceleration portion of the test; during descent from 139 000 to 115 000 feet (42.4 to 35.1 kilometers), the average magnitude of the resultant displacement from the local vertical was less than 10° .

7. The parachute was of sufficient strength to withstand the loads encountered in that no damage was sustained during the test.

8. A postflight examination of the parachute indicated that the preflight sterilization heat cycle caused some shrinkage in the physical size of the canopy.

Langley Research Center,

National Aeronautics and Space Administration,

Langley Station, Hampton, Va., March 26, 1968,

709-08-00-01-23.

REFERENCES

1. McFall, John C., Jr.; and Murrow, Harold N.: Parachute Testing at Altitudes Between 30 and 90 Kilometers. *J. Spacecraft Rockets (Eng. Notes)*, vol. 4, no. 6, June 1967, pp. 796-798.
2. Eckstrom, Clinton V.; and Preisser, John S.: Flight Test of a 30-Foot-Nominal-Diameter Disk-Gap-Band Parachute Deployed at a Mach Number of 1.56 and a Dynamic Pressure of 11.4 Pounds Per Square Foot. NASA TM X-1451, 1967.
3. Bendura, Richard J.; Huckins, Earle K., III; and Coltrane, Lucille C.: Performance of a 19.7-Meter-Diameter Disk-Gap-Band Parachute in a Simulated Martian Environment. NASA TM X-1499, 1967.
4. Whitlock, Charles H.; Bendura, Richard J.; and Coltrane, Lucille C.: Performance of a 26-Meter-Diameter Ringsail Parachute in a Simulated Martian Environment. NASA TM X-1356, 1967.
5. Preisser, John S.; Eckstrom, Clinton V.; and Murrow, Harold N.: Flight Test of a 31.2-Foot-Diameter Modified Ringsail Parachute Deployed at a Mach Number of 1.39 and a Dynamic Pressure of 11.0 Pounds Per Square Foot. NASA TM X-1414, 1967.
6. Eckstrom, Clinton V.; Murrow, Harold N.; and Preisser, John S.: Flight Test of a 40-Foot-Nominal-Diameter Modified Ringsail Parachute Deployed at a Mach Number of 1.64 and a Dynamic Pressure of 9.1 Pounds Per Square Foot. NASA TM X-1484, 1967.
7. Whitlock, Charles H.; Henning, Allen B.; and Coltrane, Lucille C.: Performance of a 16.6-Meter-Diameter Modified Ringsail Parachute in a Simulated Martian Environment. NASA TM X-1500, 1968.
8. Preisser, John S.; and Eckstrom, Clinton V.: Flight Test of a 30-Foot-Nominal-Diameter Cross Parachute Deployed at a Mach Number of 1.57 and a Dynamic Pressure of 9.7 Pounds Per Square Foot. NASA TM X-1542, 1968.
9. Lundstrom, Reginald R.; Darnell, Wayne L.; and Coltrane, Lucille C.: Performance of a 16.6-Meter-Diameter Cross Parachute in a Simulated Martian Environment. NASA TM X-1543, 1968.

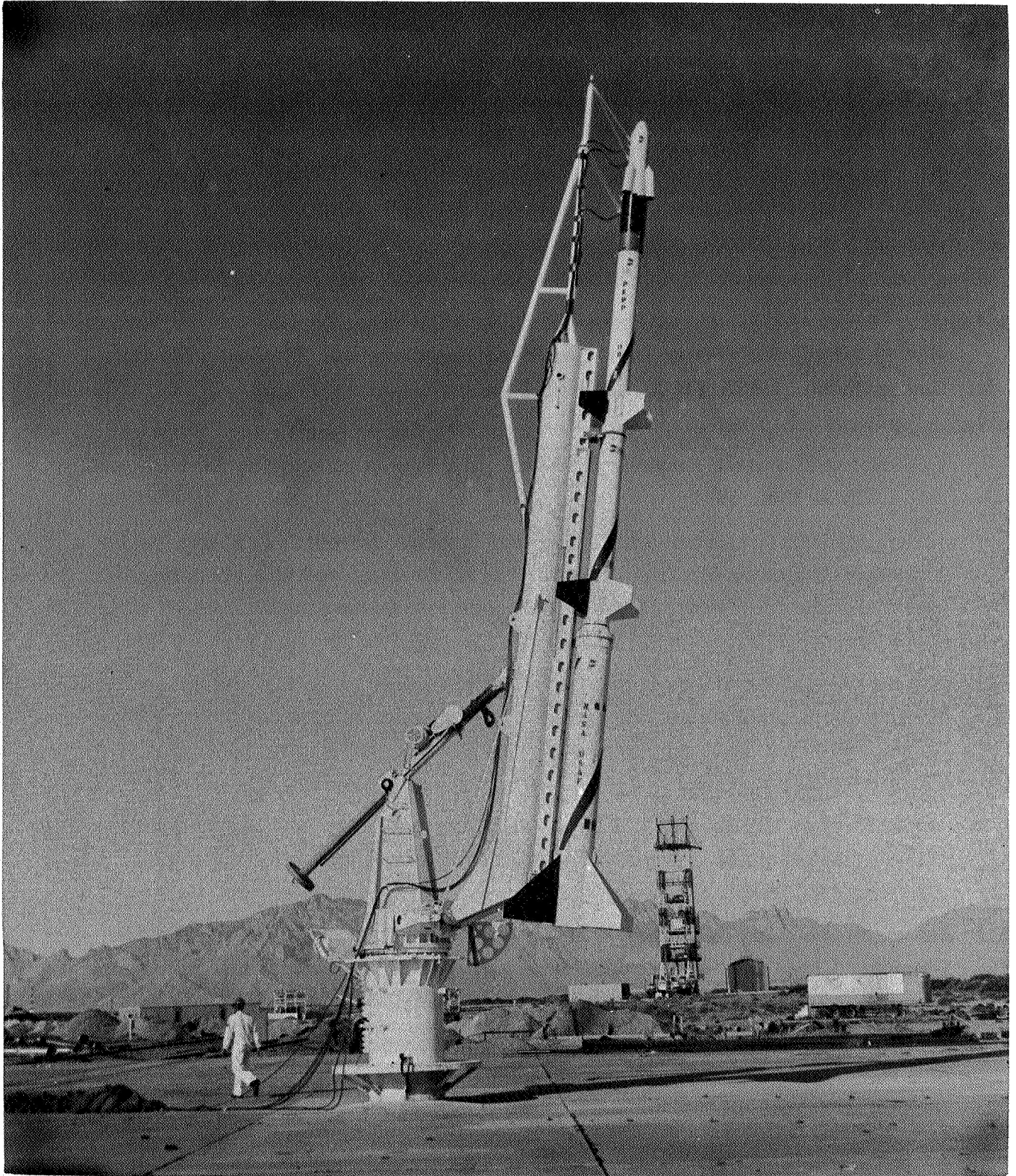
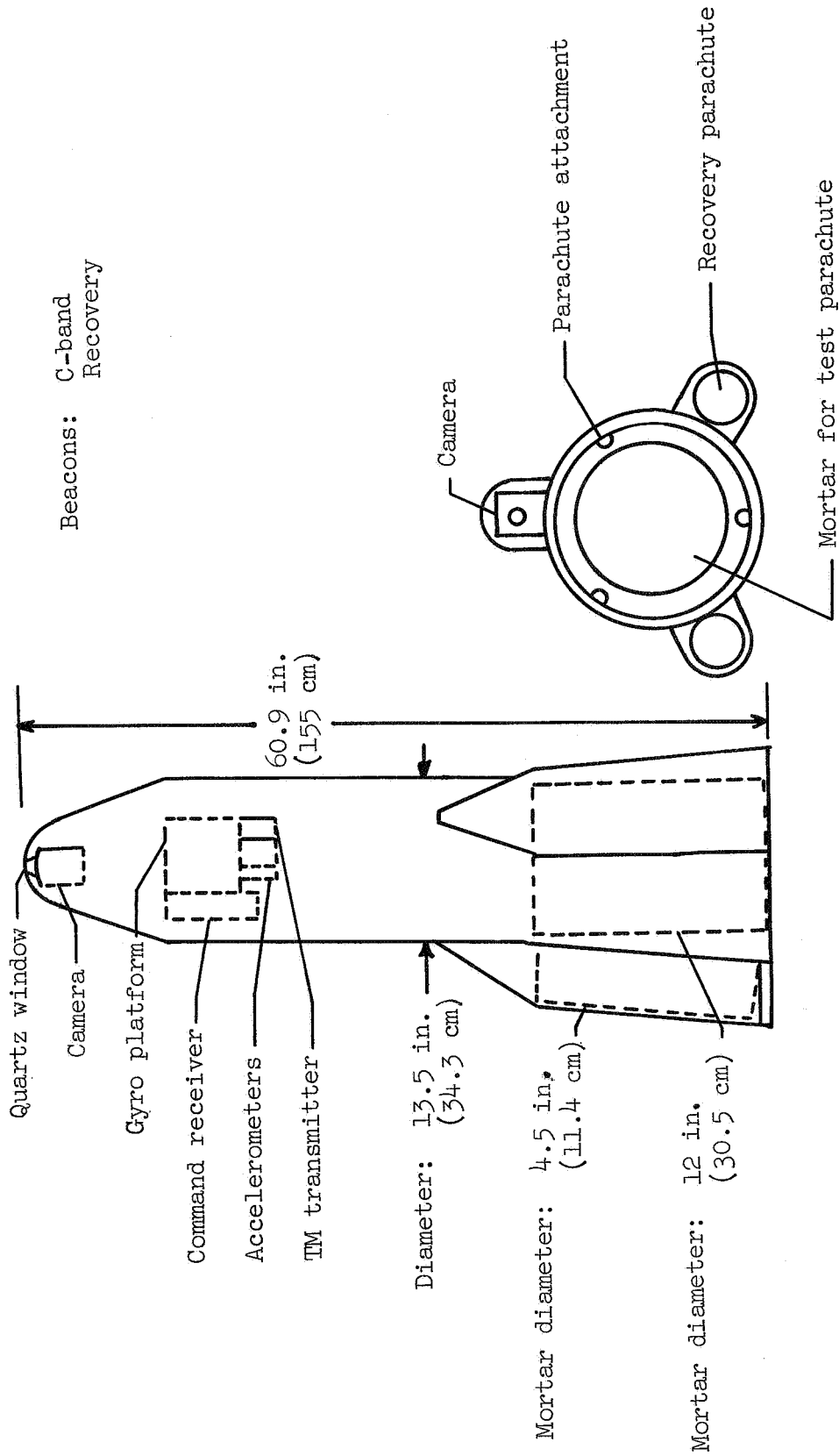


Figure 1.- Photograph of vehicle configuration.

L-68-867



Side view

Aft end view

Figure 2.- Test payload.

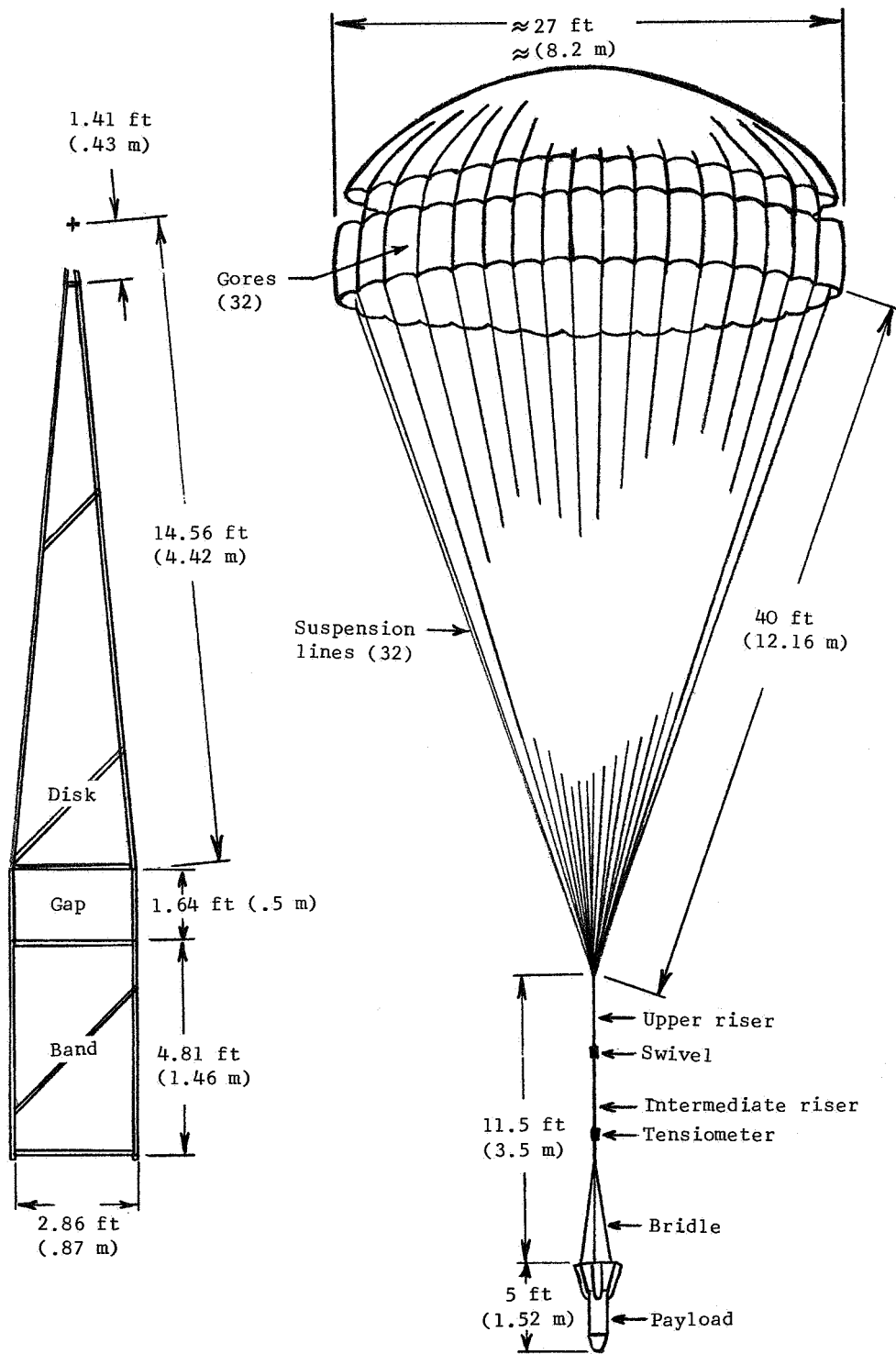
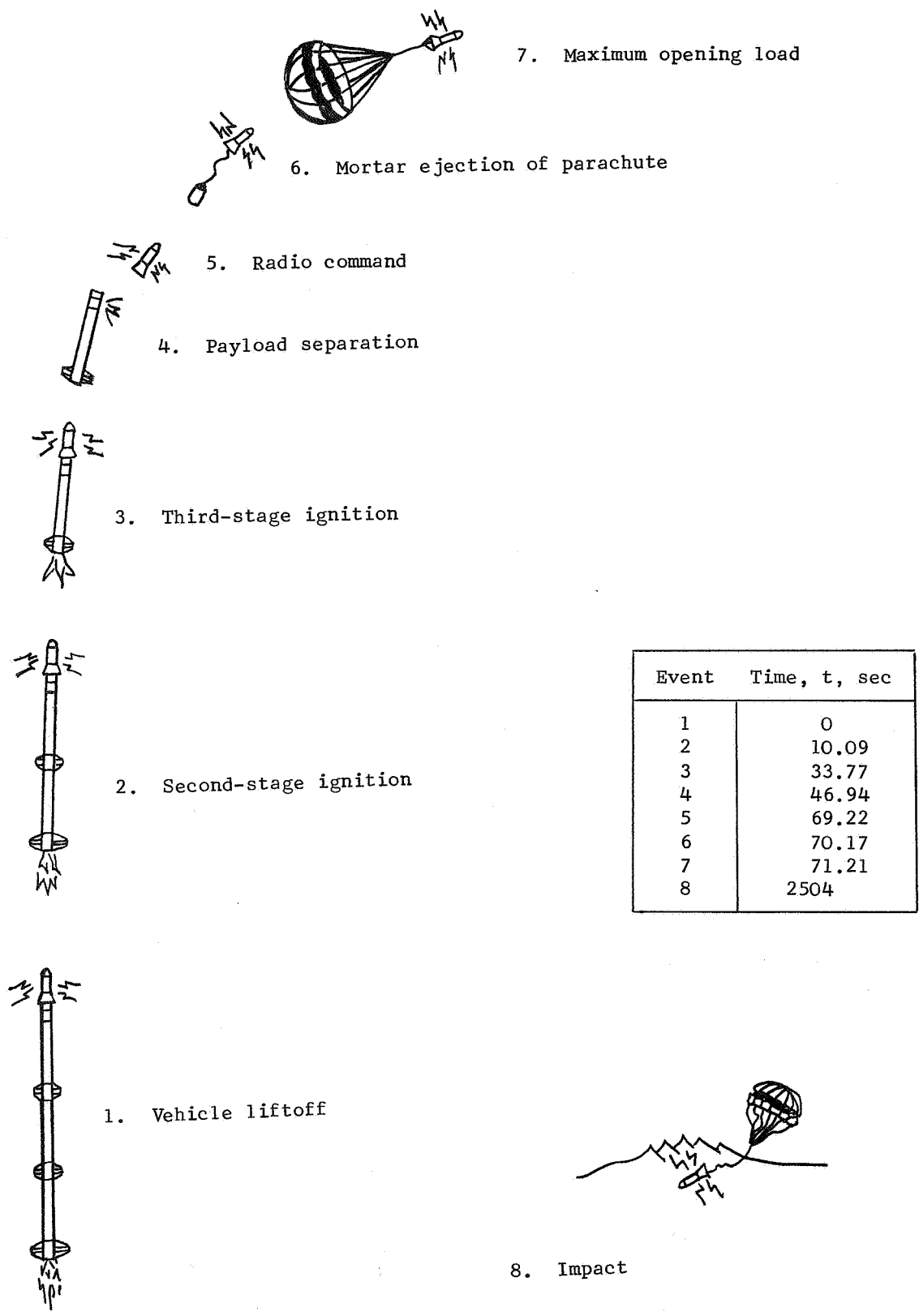


Figure 3.- Parachute-gore dimensional details and flight configuration.



7. Maximum opening load

6. Mortar ejection of parachute

5. Radio command

4. Payload separation

3. Third-stage ignition

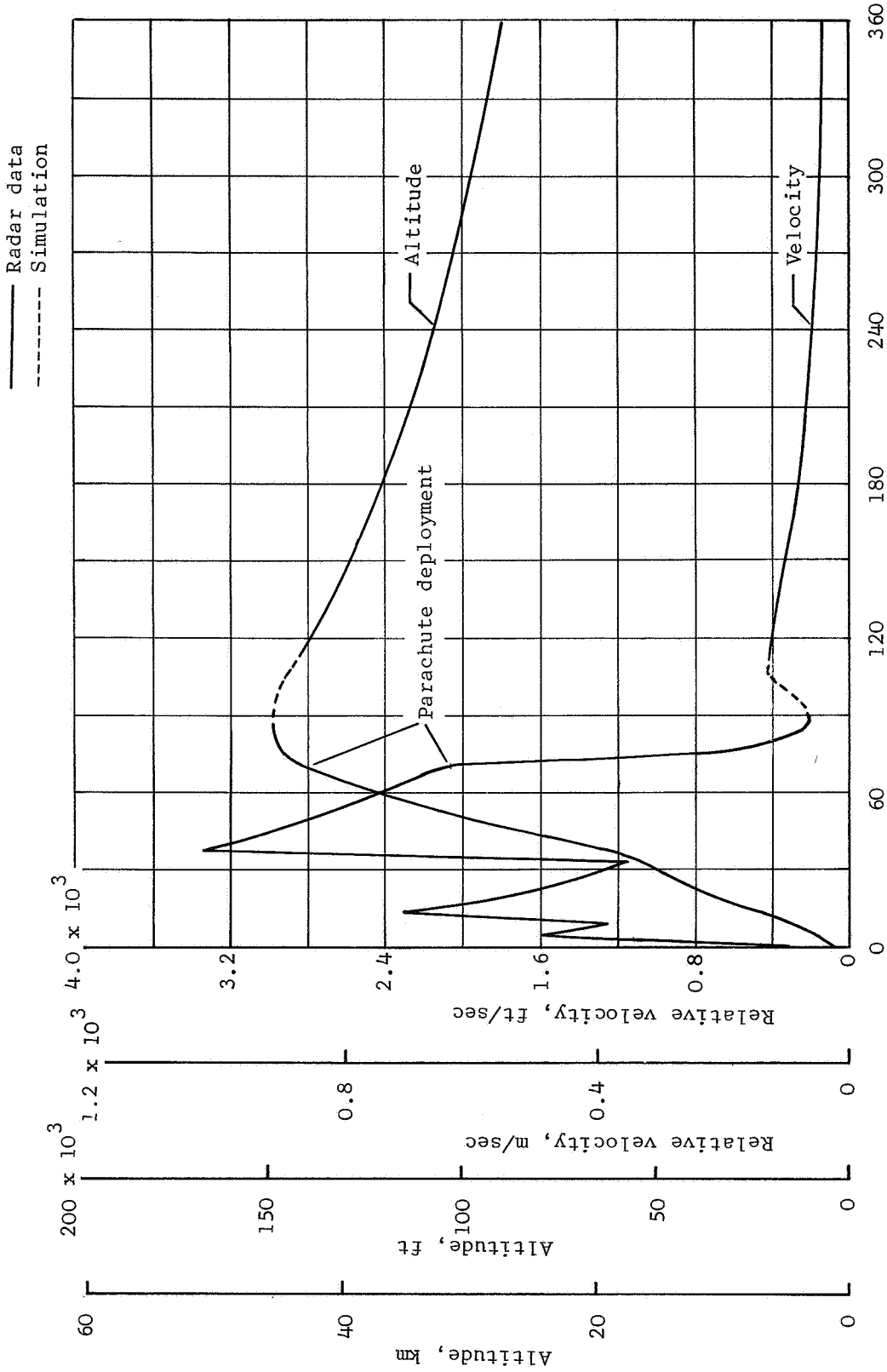
2. Second-stage ignition

1. Vehicle liftoff

8. Impact

Event	Time, t, sec
1	0
2	10.09
3	33.77
4	46.94
5	69.22
6	70.17
7	71.21
8	2504

Figure 4.- Flight sequence of events.



Time from liftoff, t, sec

Figure 5.- Time histories of altitude and relative velocity.

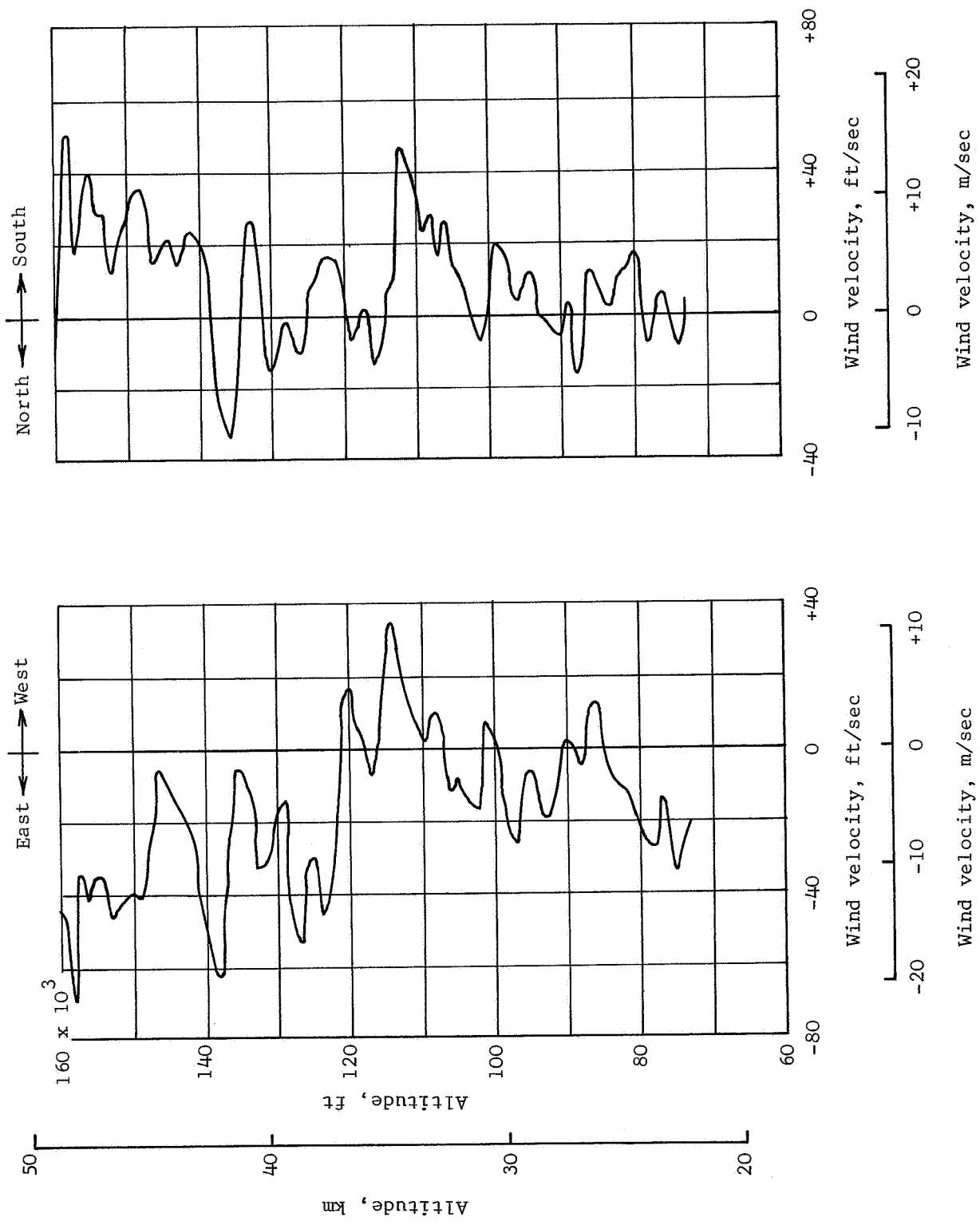


Figure 6.- Wind velocity profile in east-west and north-south components.

○ Meteorological sounding rocket data
 □ Rawinsonde data
 --- 1962 U.S. Standard Atmosphere

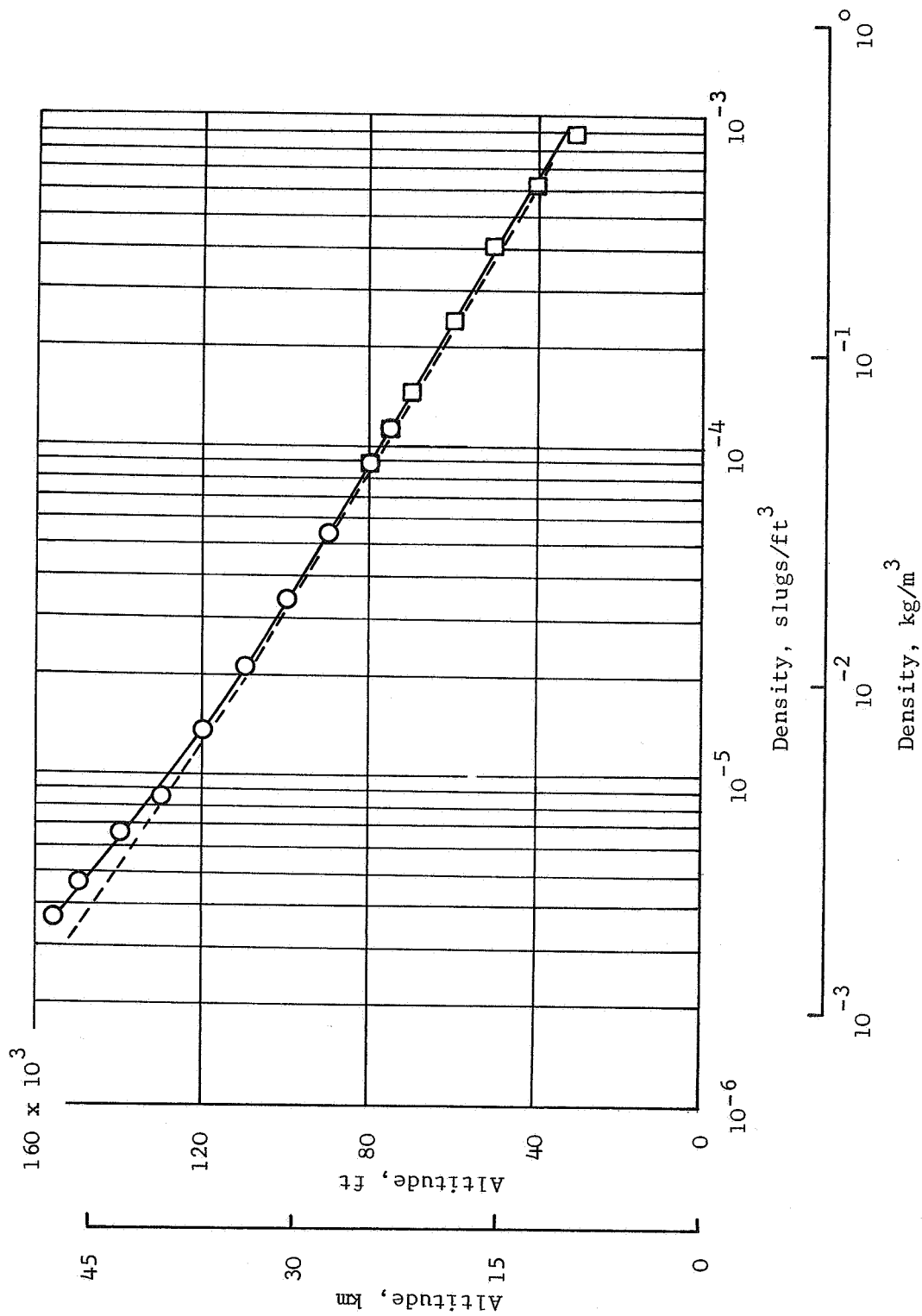
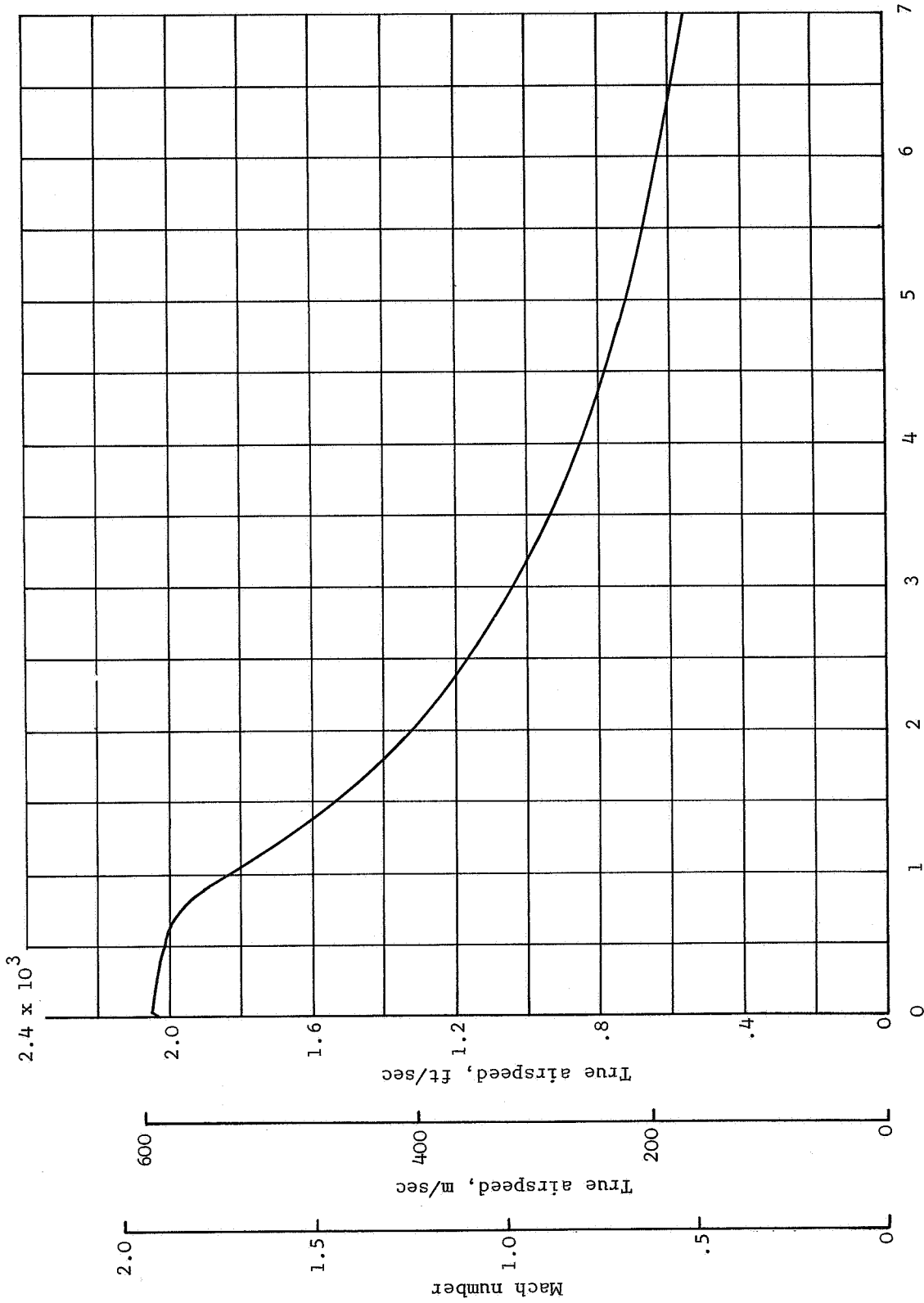
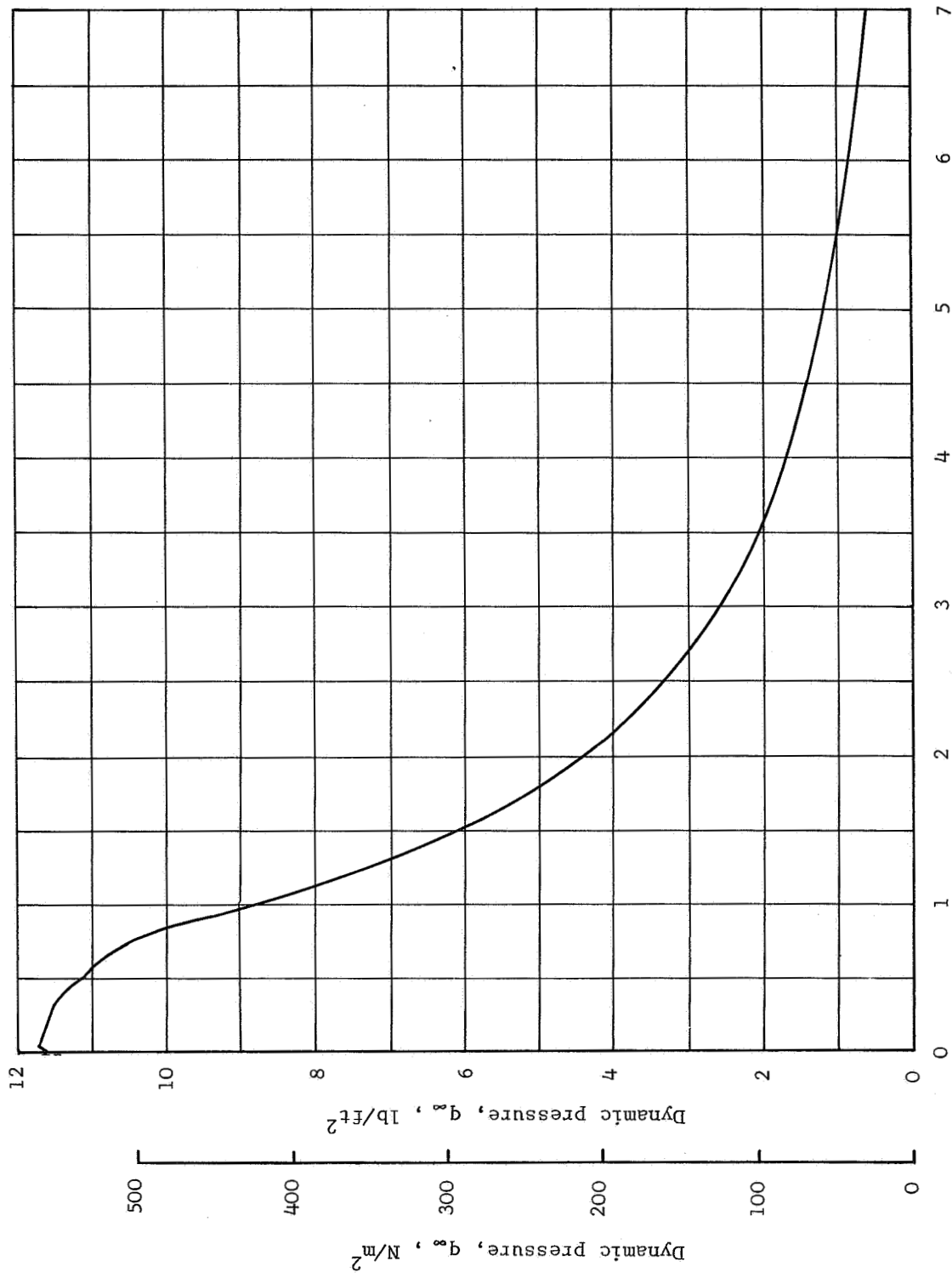


Figure 7.- Atmospheric density profile.



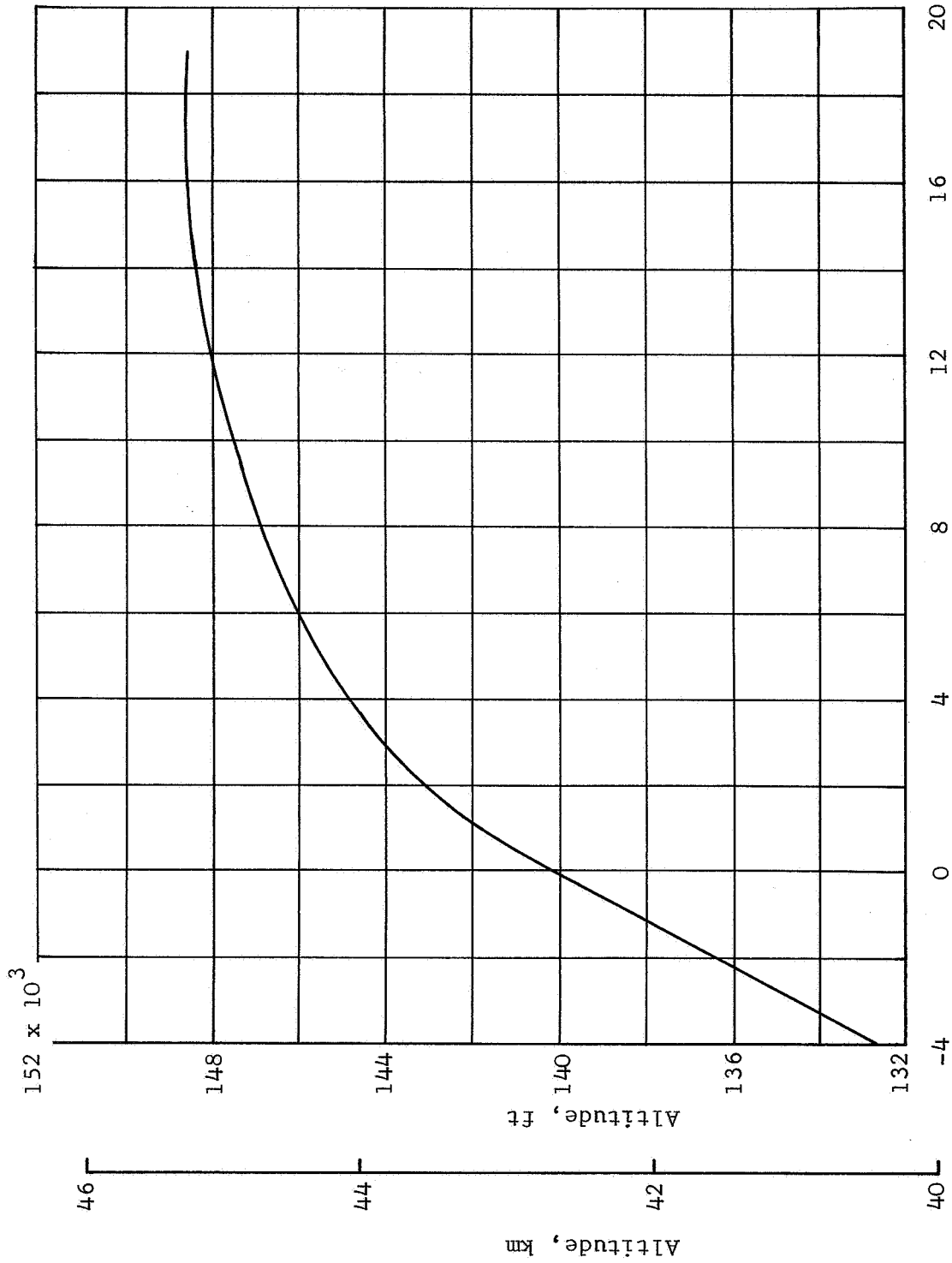
Time from mortar firing, t', sec

Figure 8.- Mach number and true airspeed time histories.



Time from mortar firing, t' , sec

Figure 9.- Dynamic-pressure time history.



Time from mortar firing, t', sec

Figure 10.- Altitude time history.

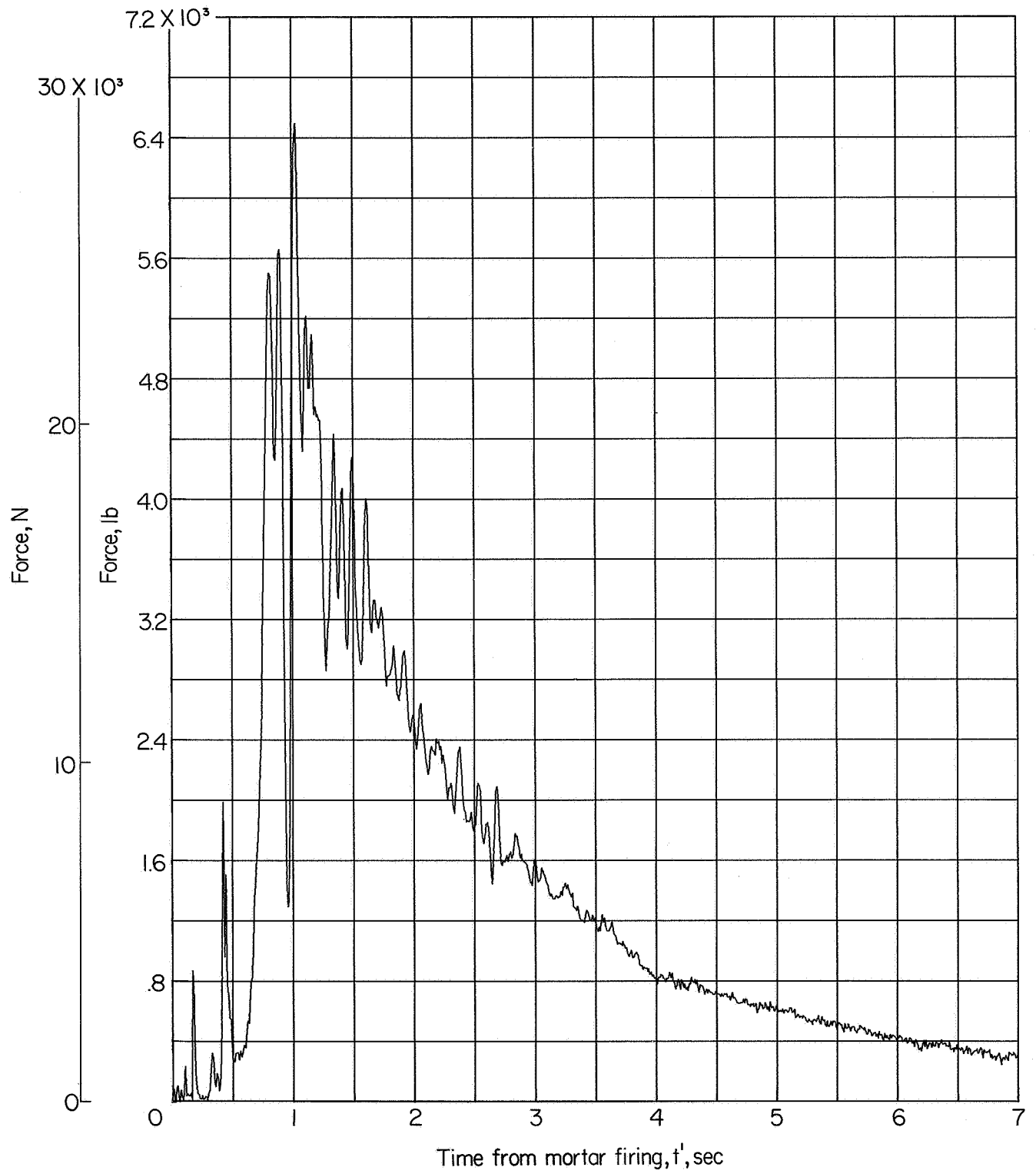


Figure 11.- Time history of force measured by the tensiometer.

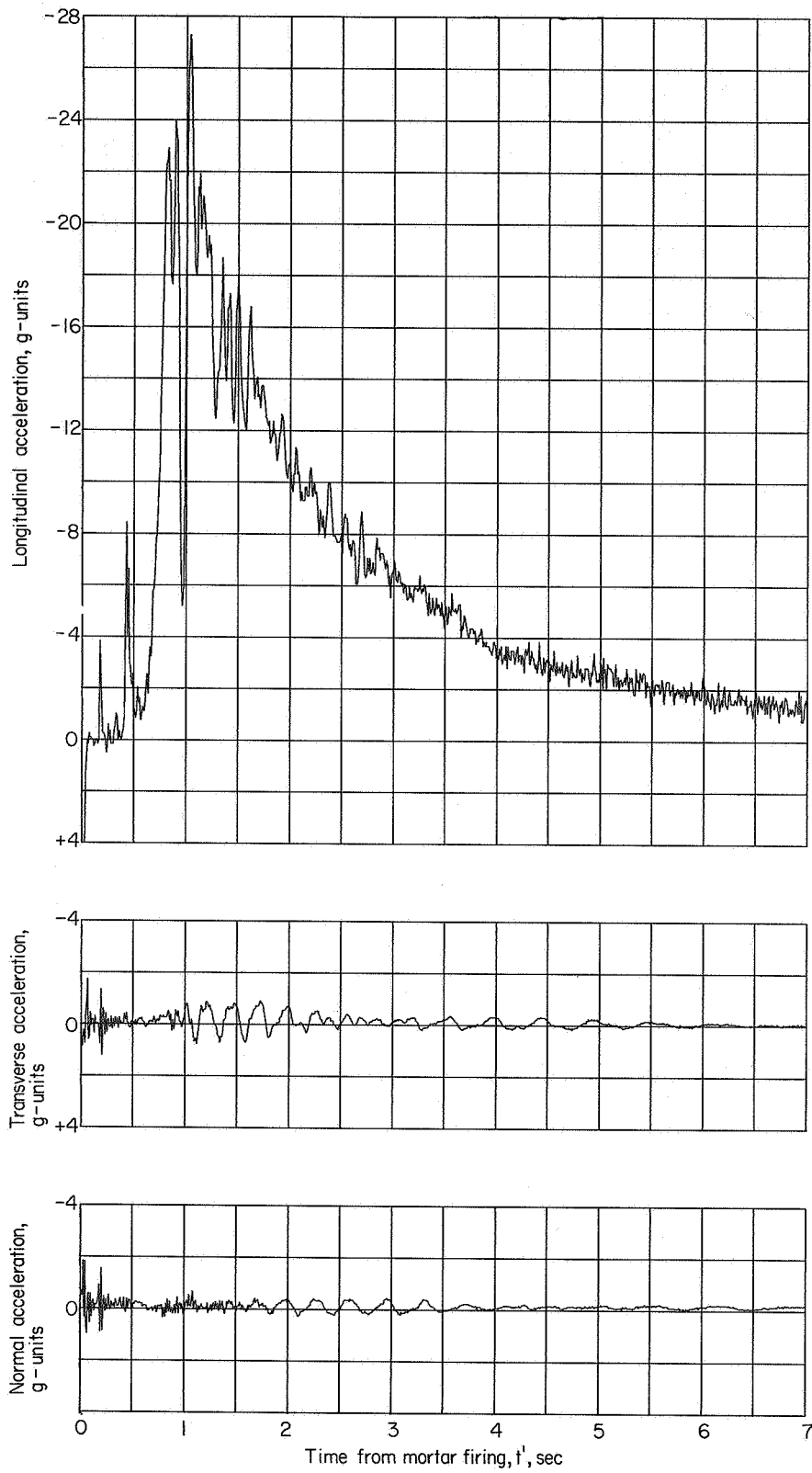
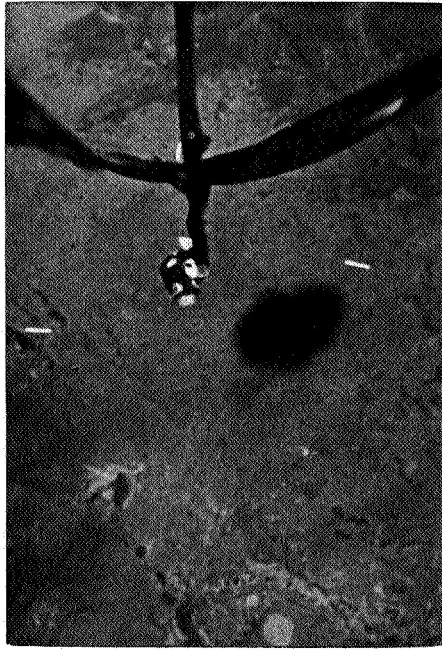


Figure 12.- Acceleration time histories.



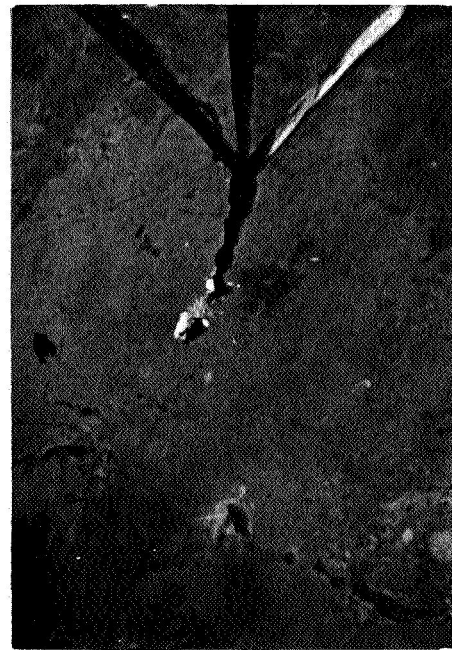
$t' = 0.19 \text{ sec}$



$t' = 0.26 \text{ sec}$



$t' = 0.32 \text{ sec}$

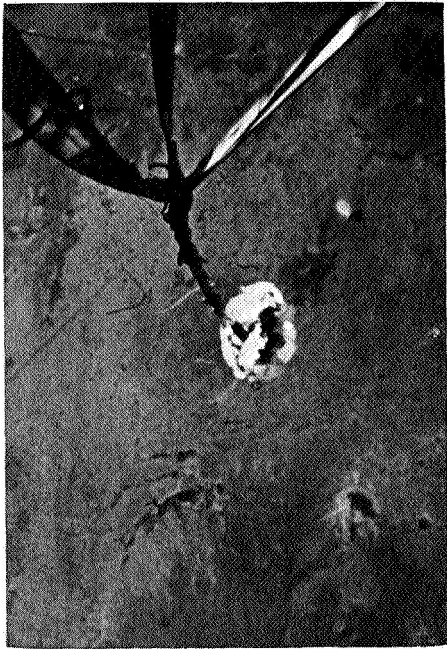


$t' = 0.45 \text{ sec}$

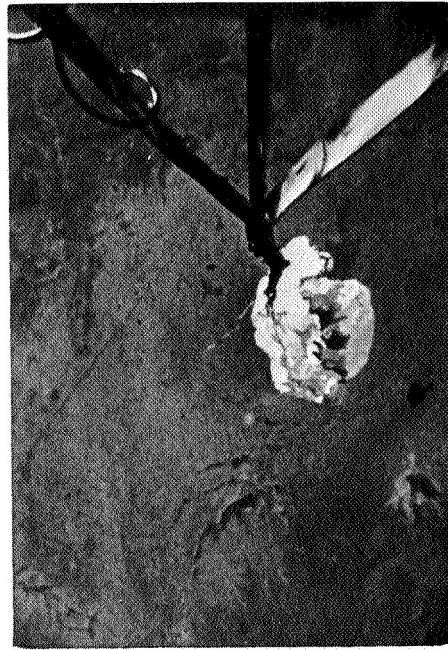
(a) Deployment.

L-68-868

Figure 13.- Onboard camera photographs.



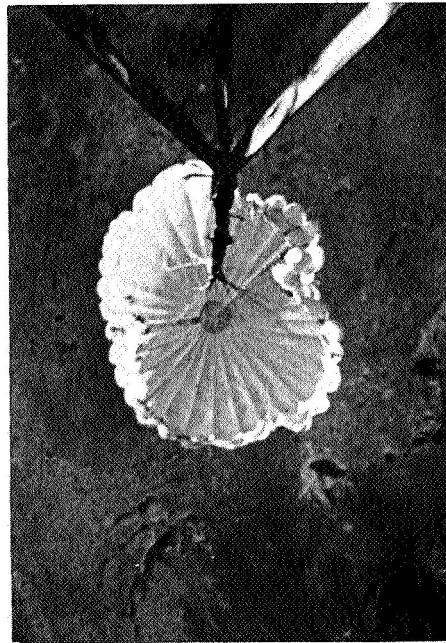
$t^* = 0.58 \text{ sec}$



$t^* = 0.64 \text{ sec}$



$t^* = 0.70 \text{ sec}$

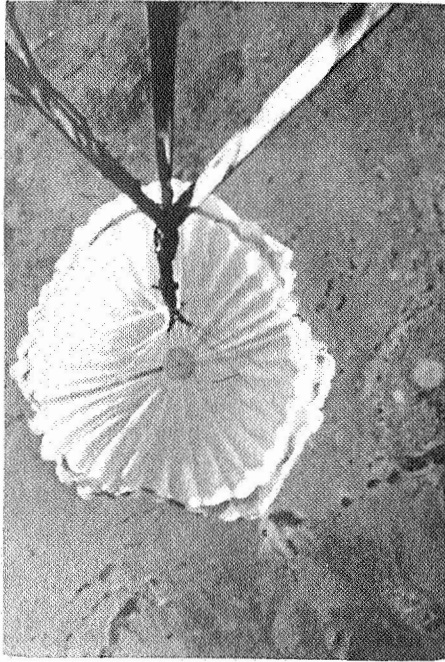


$t^* = 0.77 \text{ sec}$

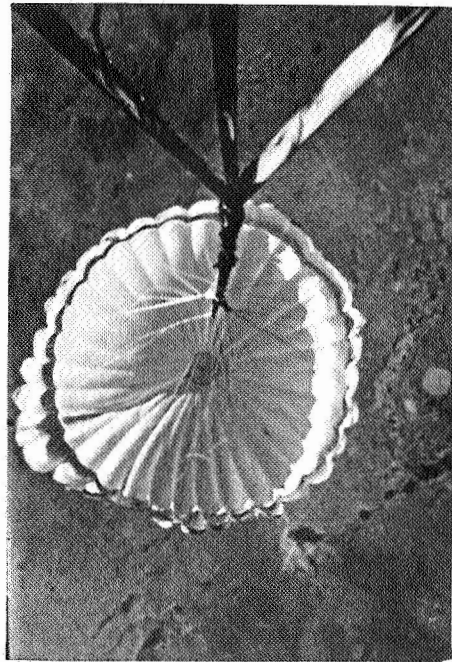
(b) Canopy inflation sequence.

L-68-869

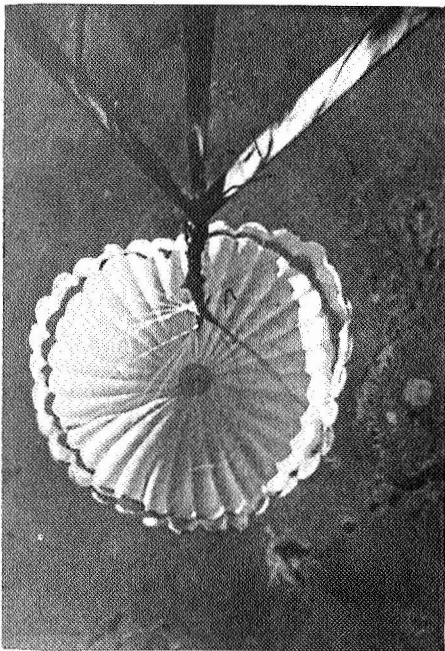
Figure 13.- Continued.



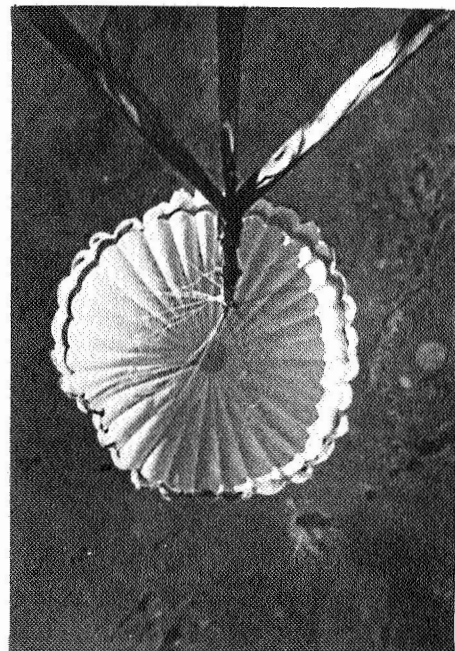
$t' = 0.80 \text{ sec}$



$t' = 0.83 \text{ sec}$



$t' = 0.86 \text{ sec}$

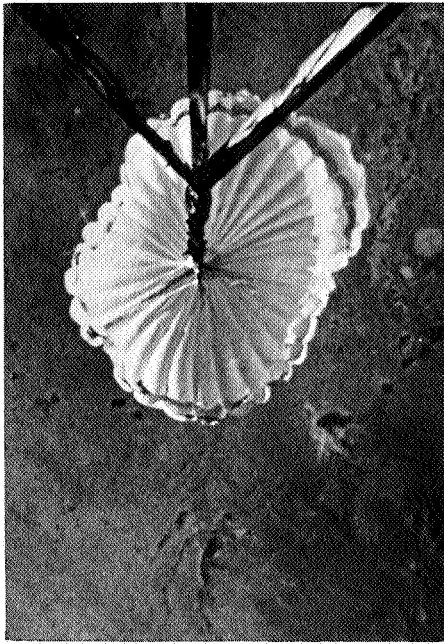


$t' = 0.90 \text{ sec}$

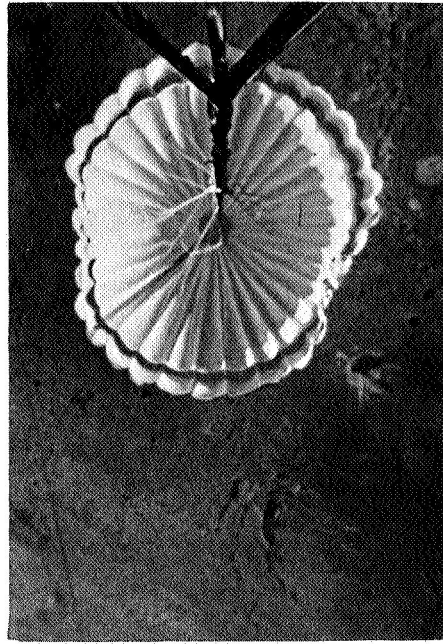
(b) Continued.

L-68-870

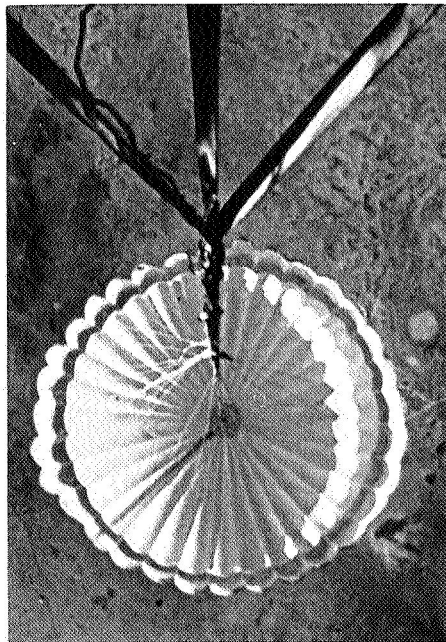
Figure 13.- Continued.



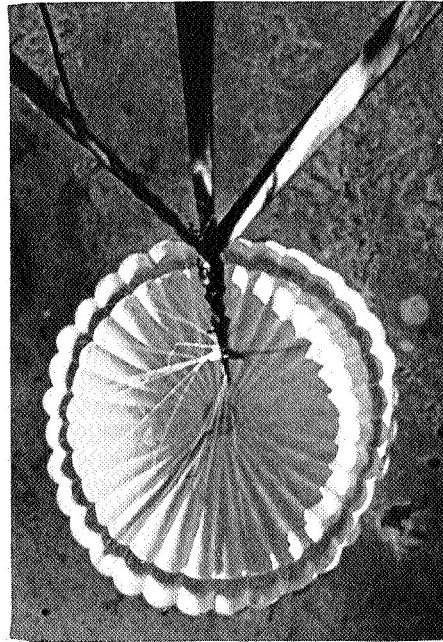
$t' = 0.96 \text{ sec}$



$t' = 1.02 \text{ sec}$



$t' = 1.09 \text{ sec}$

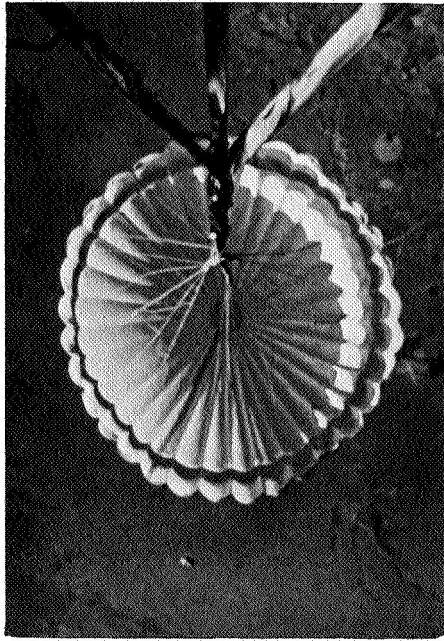


$t' = 1.12 \text{ sec}$

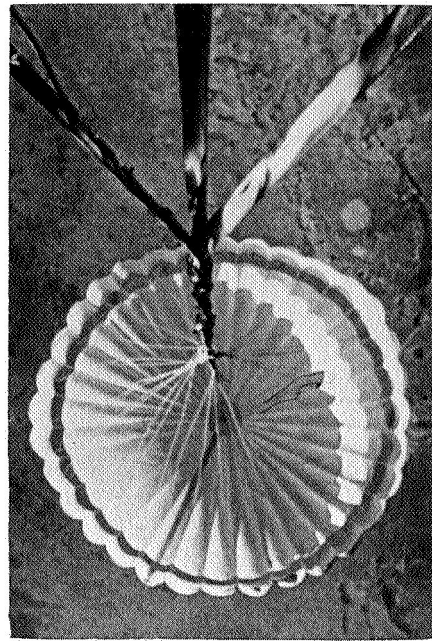
(b) Concluded.

L-68-871

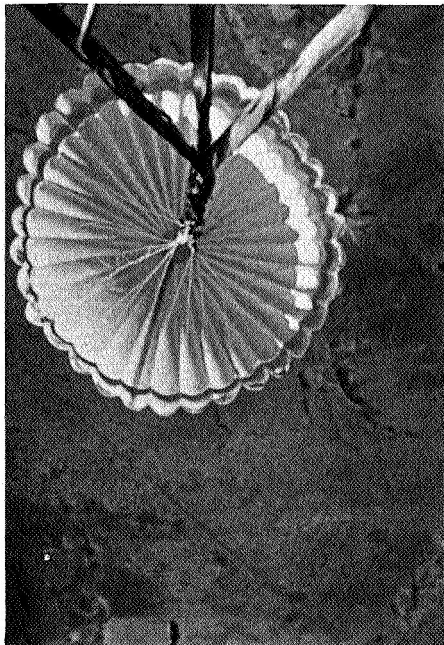
Figure 13.- Continued.



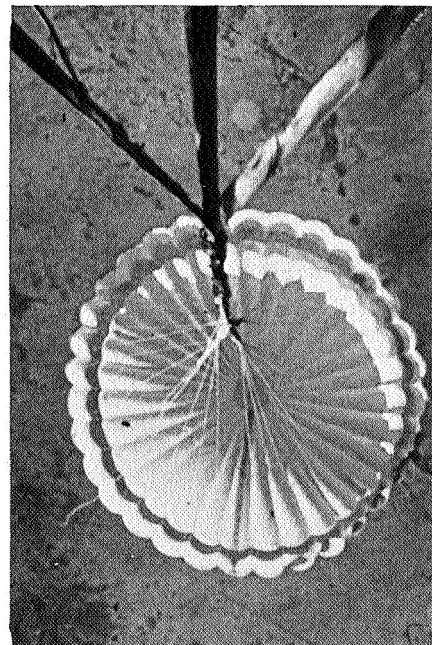
$t' = 1.28 \text{ sec}$



$t' = 1.35 \text{ sec}$



$t' = 1.44 \text{ sec}$

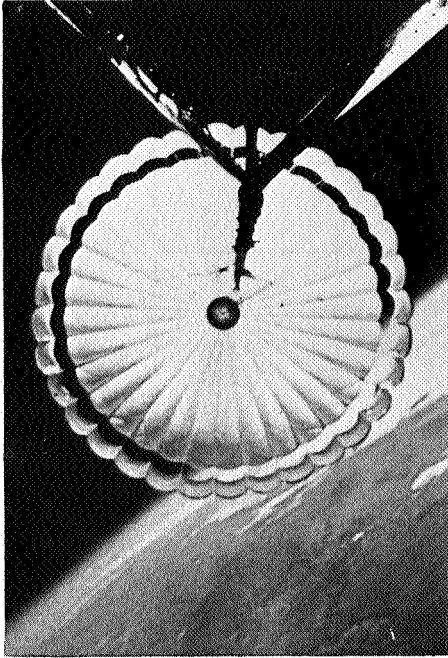


$t' = 1.57 \text{ sec}$

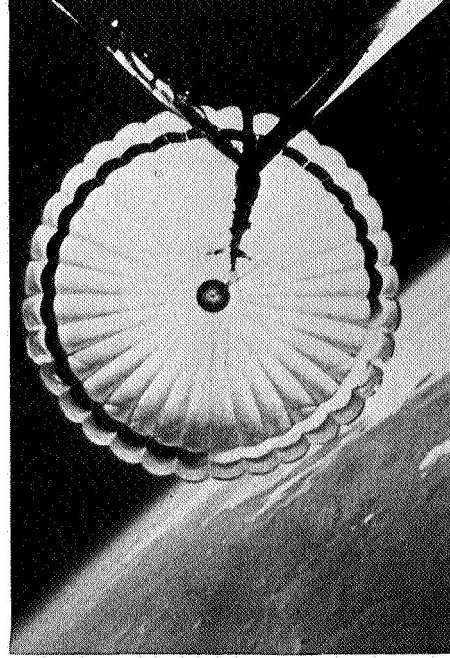
(c) Canopy band flutter.

L-68-872

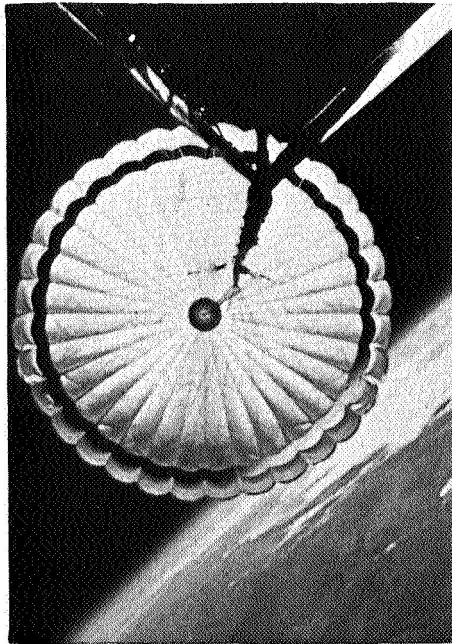
Figure 13.- Continued.



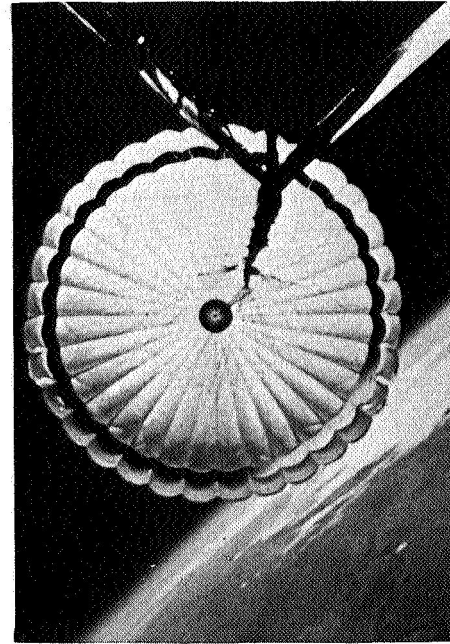
$t' = 20.09 \text{ sec}$



$t' = 20.12 \text{ sec}$



$t' = 20.15 \text{ sec}$

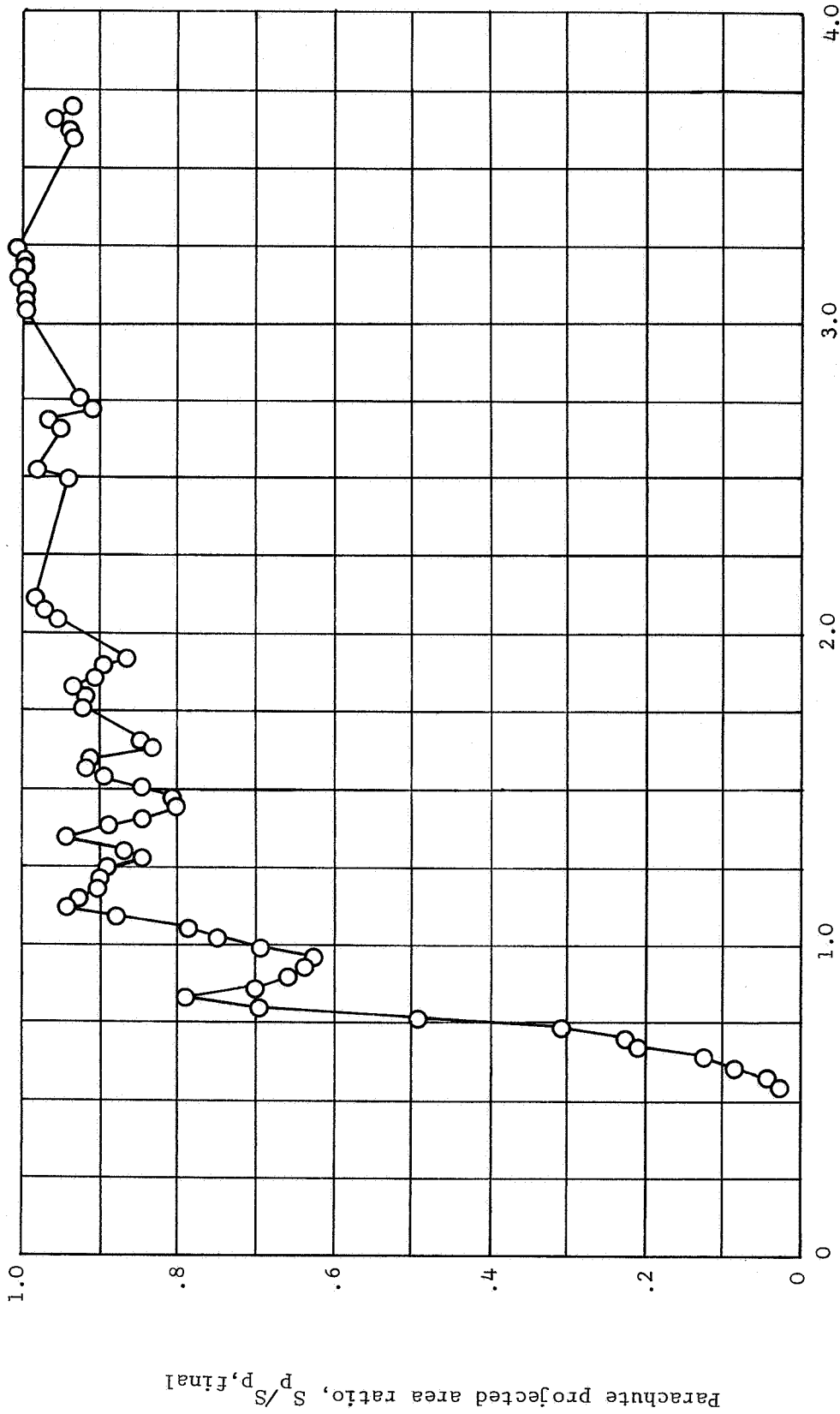


$t' = 20.18 \text{ sec}$

(d) Parachute at apogee.

L-68-873

Figure 13.- Concluded.



Time from mortar firing, t' , sec

Figure 14.- Parachute projected-area-ratio time history.

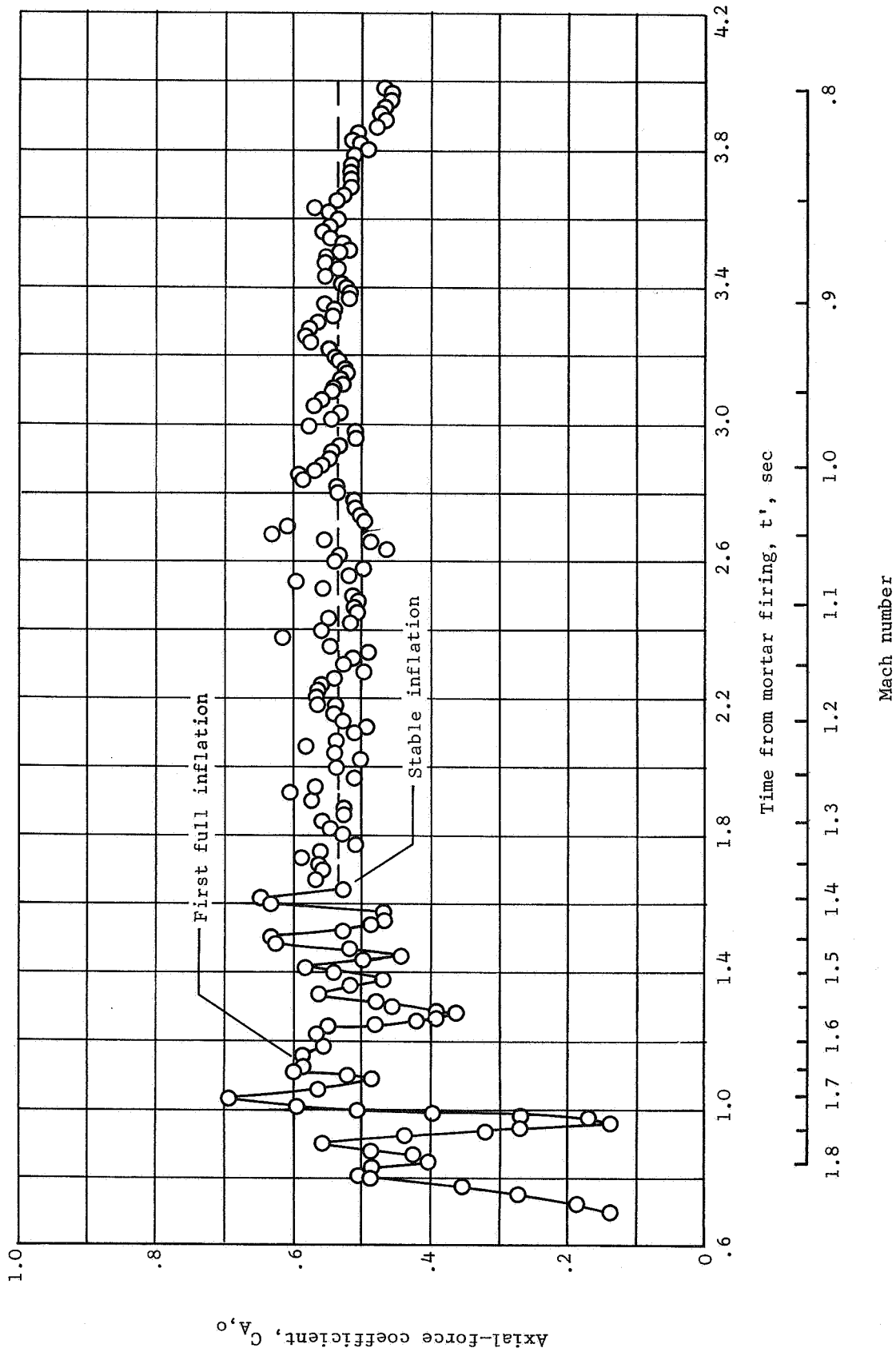


Figure 15.- Variation of axial-force coefficient with time and Mach number.

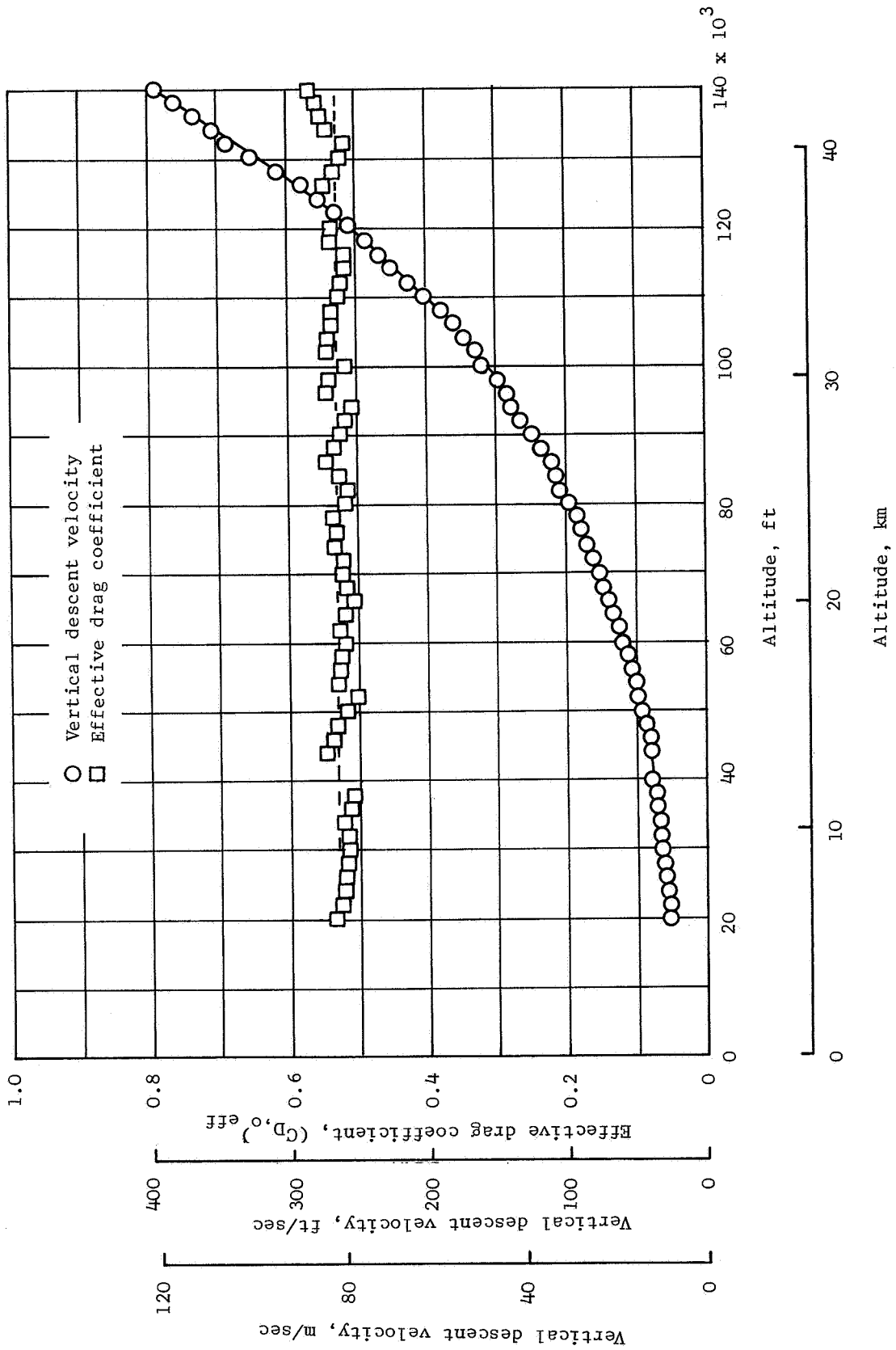
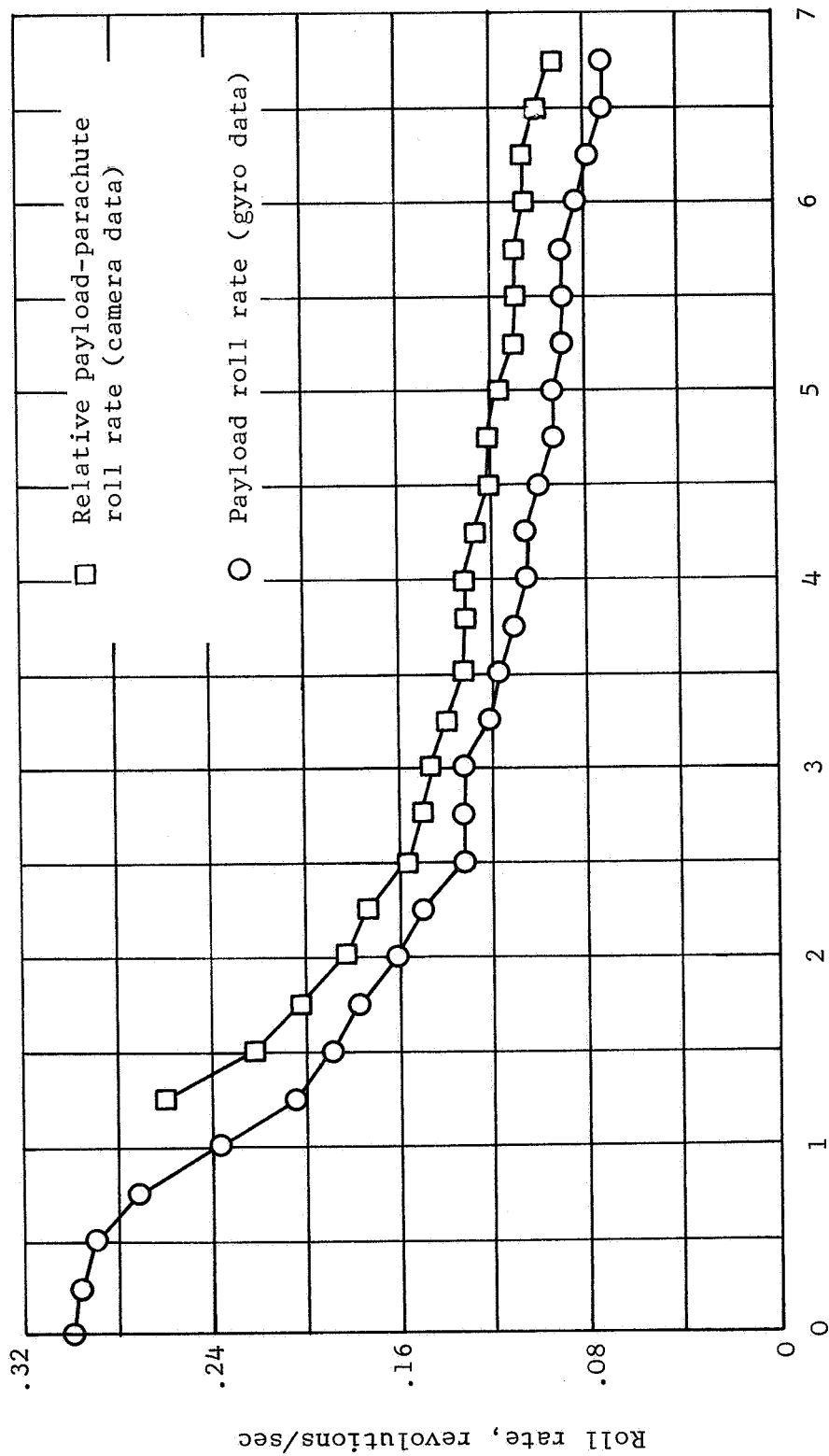
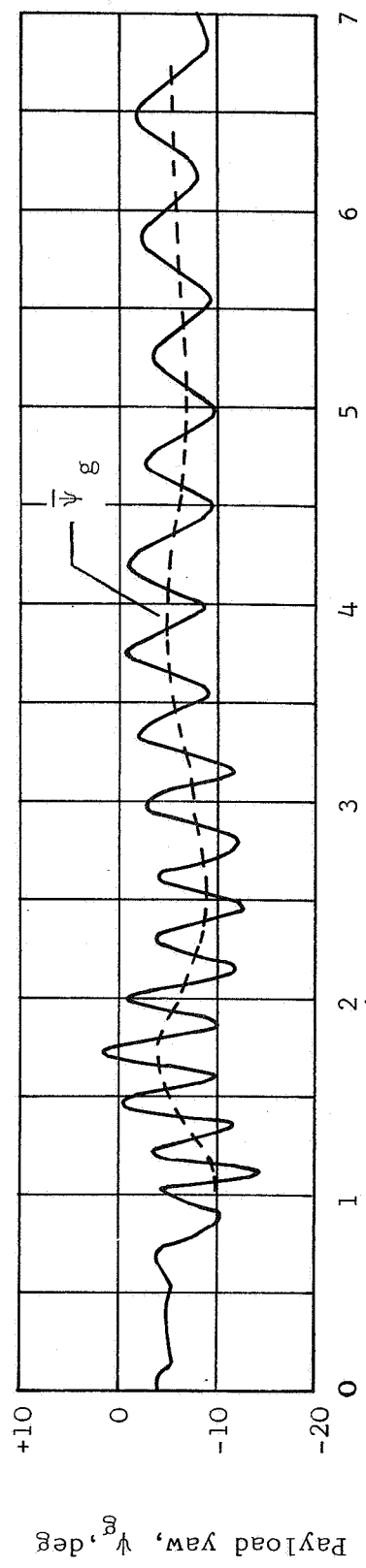
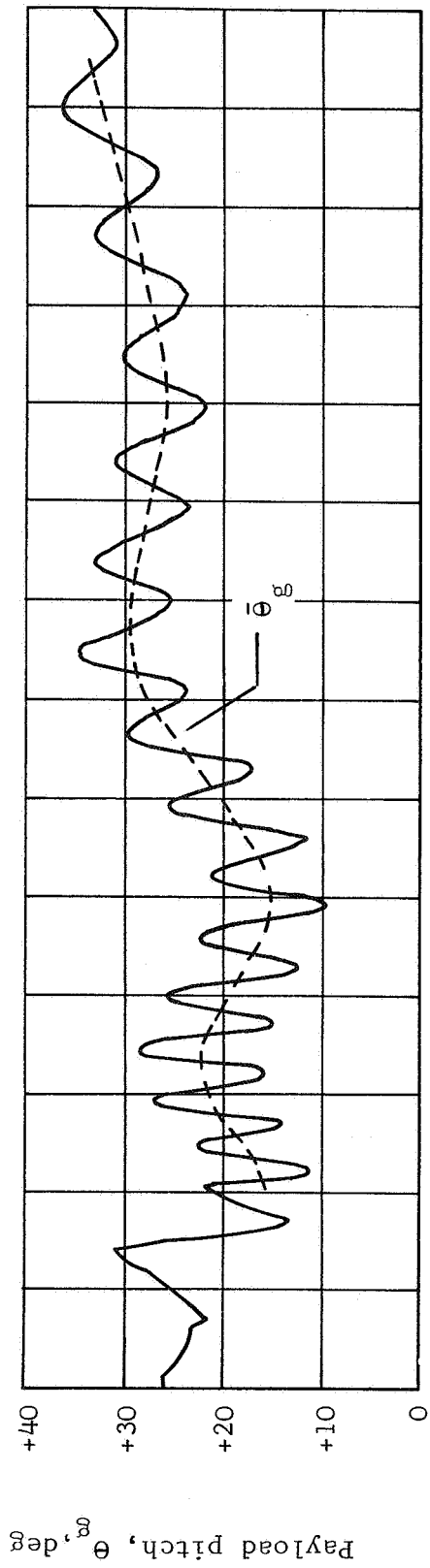


Figure 16.- Variation of vertical descent velocity and effective drag coefficient with altitude.



Time from mortar firing, t', sec

Figure 17.- Comparison of payload roll rate with relative payload-parachute roll rate.



Time from mortar firing, t' , sec

Figure 18.- Payload pitch and yaw angle time histories. (Pitch is measured relative to vehicle elevation at lift-off. Pitch downward is positive. Yaw is measured relative to the pitch attitude in the plane of the payload perpendicular to the pitch plane.)

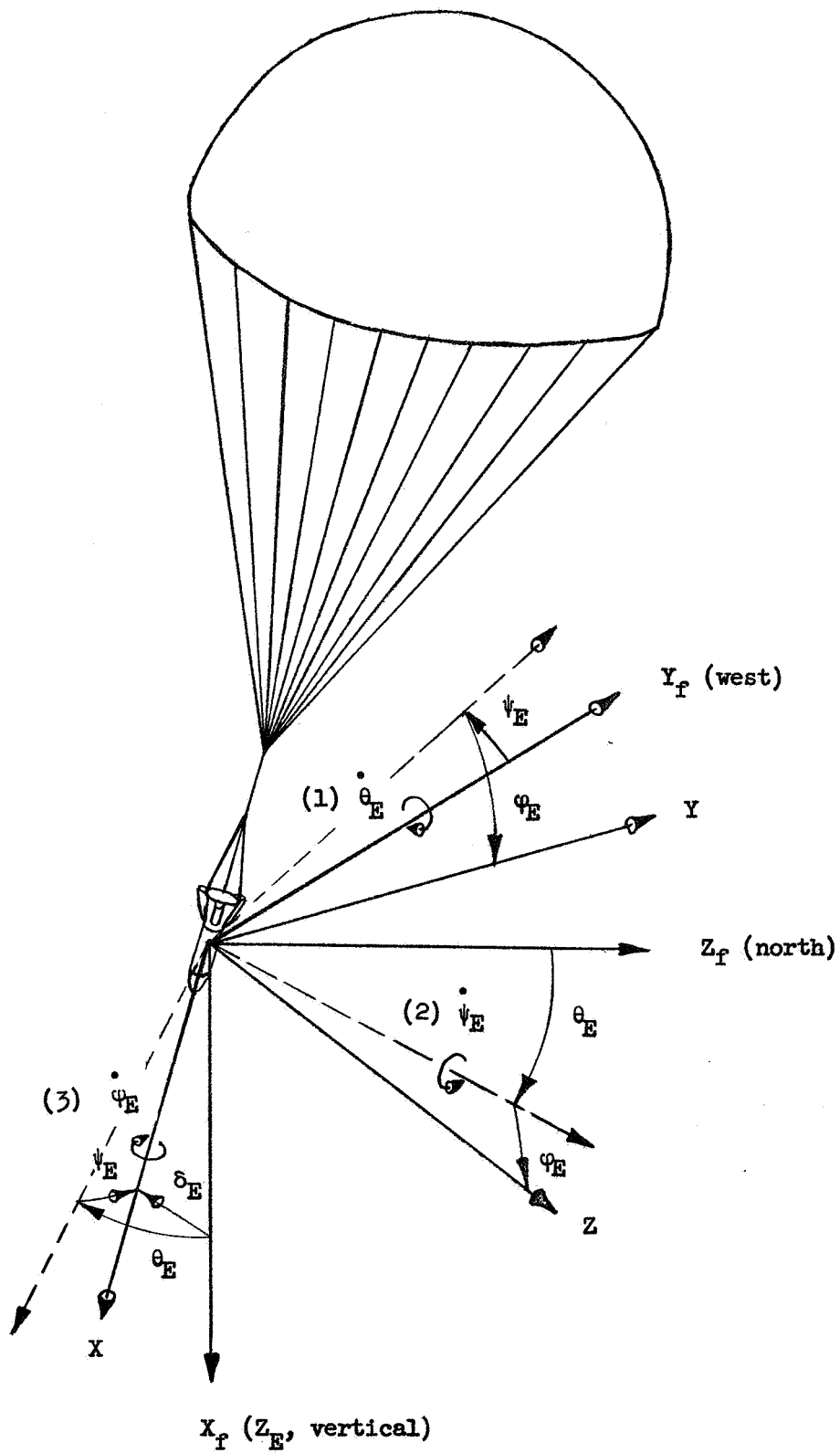
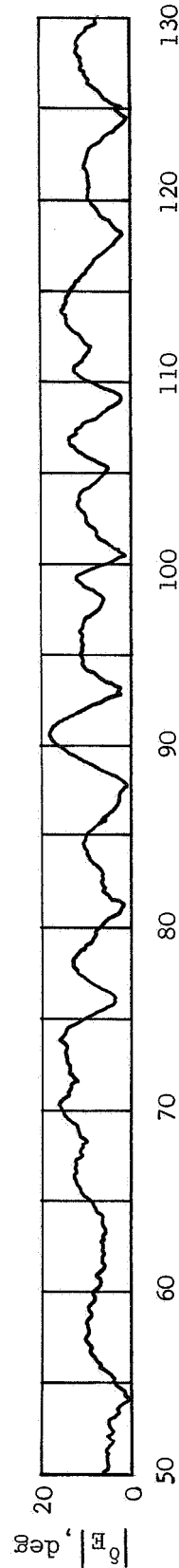
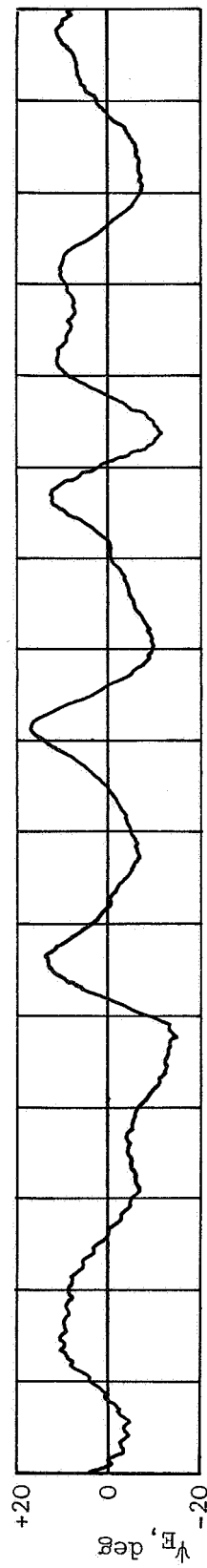
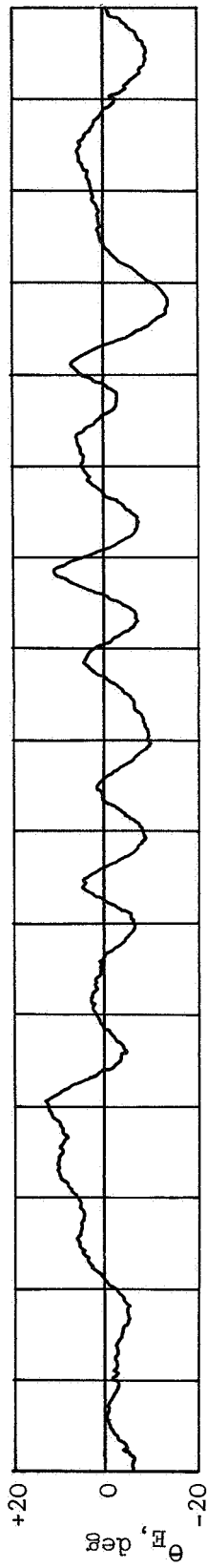


Figure 19.- Sketch showing relationship between body axes (X, Y, Z) and earth-fixed axes (X_f, Y_f, Z_f) .



Time from mortar firing, t' , sec

Figure 20.- Time histories of pitch θ_E , yaw ψ_E , and the magnitude of the resultant angular displacement δ_E of payload from the local vertical for a portion of descent from 139 000 to 115 000 feet (42.4 to 35.1 kilometers).

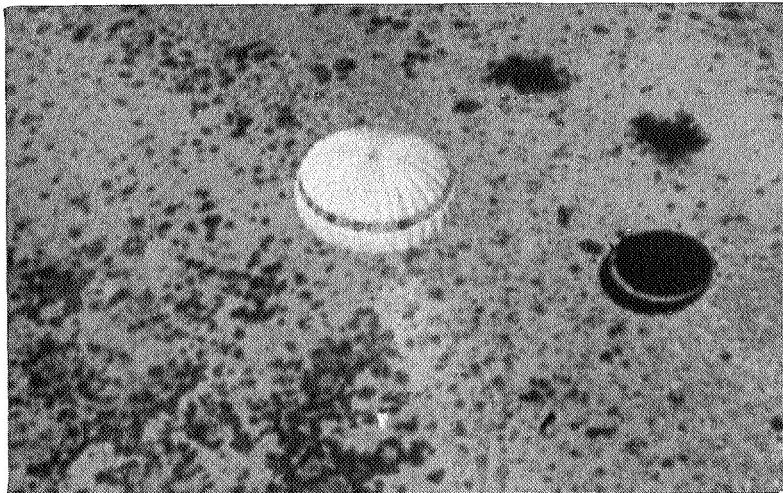
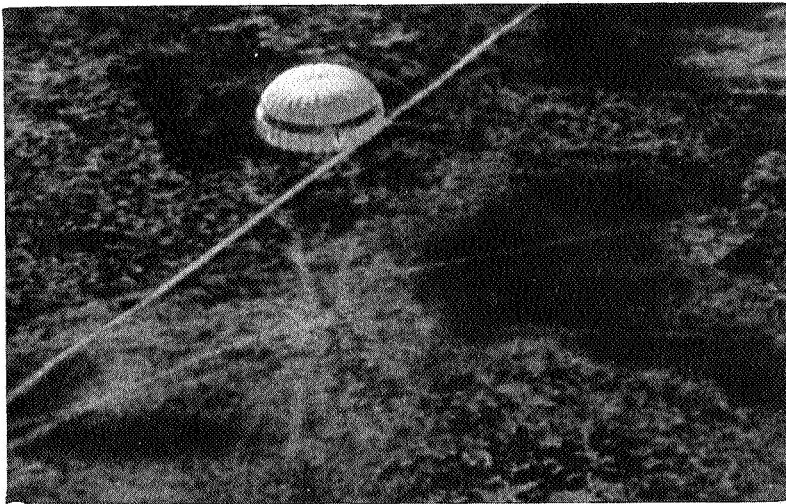
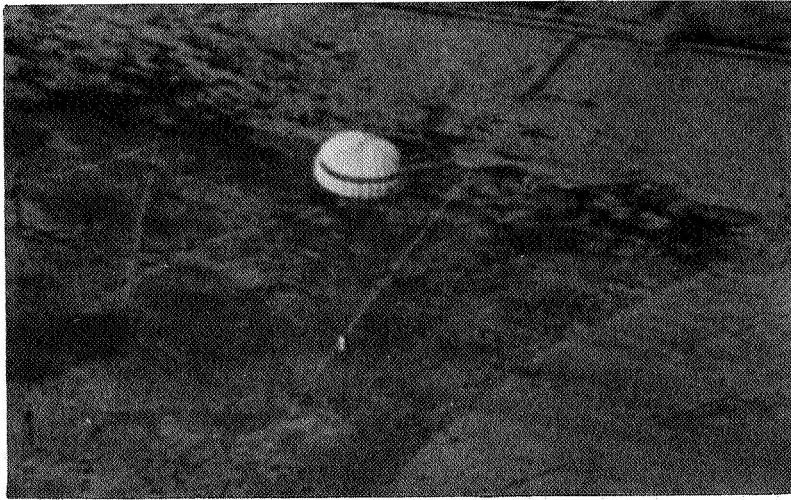


Figure 21.- Photographs of parachute during descent shortly before impact.

L-68-874

A motion-picture film supplement L-1000 is available on loan. Requests will be filled in the order received. You will be notified of the approximate date scheduled.

The film (16 mm, 7 min, color, silent) is in three sections and shows (1) the parachute during deployment, inflation, the deceleration period, and a portion of descent as taken by a camera mounted on the aft end of the payload; (2) the payload-parachute system during descent taken from telescopic cameras located on the test range; and (3) the last portion of the descent including ground impact as taken from a recovery aircraft.

Requests for the film should be addressed to:

Chief, Photographic Division
NASA Langley Research Center
Langley Station
Hampton, Va. 23365

CUT

Date _____

Please send, on loan, copy of film supplement L-1000 to
TM X-1575

Name of organization

Street number

City and State Zip code

Attention: Mr. _____
Title _____

Place
Stamp
Here

Chief, Photographic Division
NASA Langley Research Center
Langley Station
Hampton, Va. 23365